Reviewer #1

This paper investigates the role of different weather conditions in modulating summertime boundary layer and further surface pollution in Beijing. A novel technique is applied to classify summertime circulation patterns into seven major weather types. More importantly, the authors thoroughly investigated the mechanism how different synoptic conditions impact on the variability of boundary layer height and structure, which is the major factor governing the vertical transport of pollutants and thus surface pollution level. The paper is also well presented and logically organized. I think this paper addresses an important issue and makes great contribution to our understanding of summer haze in Beijing. I thus recommend the paper be accepted for publication in ACP only with several minor comments.

First of all, we appreciate tremendously the reviewer's positive comments. In response to the reviewer's comments, we have made relevant revisions to the manuscript. Listed below are our responses and the corresponding changes made to the manuscript according to suggestions given by the reviewer. Each comment of the reviewer (in black) is listed, followed by our responses (in blue).

Specific comments:

1. The introduction seems too long (4 pages). I think it could be shortened with an emphasize on the relationship between summer time boundary layer height and pollution in Beijing, and the novel method and data used in this study.

Per your suggestion, the introduction was shortened in this revision. Besides, several important literatures were added to the introduction as suggested by reviewer #2 to give a more comprehensive overview of current research and highlight the importance of this study as well.

2. Section 2.3: While the T-mode PCA is conventionally used in classification, the oblique rotation may not be familiar to the major audience. It's better to elaborate here with some mathematical explanation of this technique.

Per your suggestion, the following mathematical explanation with regard to T-mode PCA were added in the revised manuscript:

"To speed up the calculation of PCA, the data is split into ten subsets; and then, the principle components (PCs) obtained from each subset are projected on the rest data. The T-PCA classification based on cost733 software package includes the following steps:

(1) The data is standardized spatially. Each pattern's mean is subtracted from the data, and then the patterns are divided by their standard deviations.

(2) The data is split into ten subsets through selecting the data once every ten days. For example, the first subset consists of the 1st, 11th, 21st, 31st, etc. days, and the second subset consists of the 2nd, 12th, 22nd, 32nd, etc. days.

(3) The PCs are calculated using the singular value decomposition for each subset. And the PCs of each subset are ordered according to the magnitude of their explained variances.

(4) An oblique rotation (using direct oblimin) is applied on the PCs, employing an adaptation of the Gradient Projection Algorithm of Bernaards and Jennrich (2005). The main reason for using rotation is to facilitate the interpretation (Abdi and Williams, 2010). This transformation does not constrain the orthogonality, allowing for the PCs the freedom to better reflect the original data (Richman, 1981).

(5) The PC scores of each subset are projected onto the remaining data by solving the matrix equation: $\Phi A^T = F^T Z$, where F and Φ are matrices of PC scores and PC correlations, respectively, and Z is the full data matrix, and A are pseudo-loadings to be determined. Each day is classified with the PC (type) for which it has the highest loading.

(6) Contingency tables are finally used to compare the ten classifications, and the classification most consistent with the other nine classifications is selected as the resultant one."

3. Section 3.2: The authors identified seven dominant weather types. I wonder how is the order (No. 1-7) of these seven types determined. In traditional PCA, the modes are

2

usually ordered by the amount of variance explained**.** Here it does not seem to be the case as their frequencies of occurrence are not ordered from high to low? Perhaps some explanation would help?

Actually, the seven synoptic types (#1-7) were also determined by the amount of variance explained, which were 0.192415, 0.112347, 0.106, 0.092, 0.085, 0.079, and 0.077, respectively. To better understand the T-PCA, the detailed classification procedures were added on Page 9-10 in our revised manuscript (see our response to comment #2).

4. Also in this section, as types 1, 4 and 5 are associated with heavy pollution, I wonder if a composite analysis of these three types and the other four types would help better distinguish between their different characteristics in meteorological variables (RH, BLH, CLD, etc) and $PM_{2.5}$ concentration?

In the revised manuscript, we compared the meteorological variables and aerosol concentration of polluted synoptic types (1, 4, and 5) with that of other types (2, 3, 6, and 7), which were detailed in the newly added Table S2 in Supplementary Materials. It is noteworthy that the heavy aerosol pollution of Types 1, 4, and 5 are associated with the relatively low BLH, high RH2, high CLD, and high frequency of southerly PBL winds.

The relevant discussion was added on Page 13 in the revised manuscript.

Table S2. *Statistics of the correlation between PM2.5 concentrations and meteorological variables corresponding to the polluted synoptic types (1, 4, and 5) and other synoptic types. The meteorological variables (mean values ± one standard deviation) include 2-m temperature (T2), 2-m relative humidity (RH2), wind speed at the 925-hPa level (WS), southerly wind frequencies at the 925h-hPa level (WD), total cloud cover at 1400 BJT (CLD), and the BLH at 1400 BJT. The correlation coefficients (R) between the meteorological variable and PM2.5 concentration are also given, which are calculated based on the seven pairs of mean values for each synoptic pattern.*

#	Polluted types (1, 4, and 5)	Other types (2, 3, 6, and 7)	R (#, PM$_{2.5}$)
PM$_{2.5}$ ($\mu g\ m^{-3}$)	99.7 ± 51.9	56.8 ± 40.2	/
BLH (km)	1.17 ± 0.59	1.63 ± 0.69	-0.97*
RH2 (%)	68.1 ± 14.3	59.4 ± 14.1	0.85*
CLD (%)	92 ± 22	74 ± 36	0.84*
925-hPa WD (South) (%)	61 ± 6	49 ± 7	0.78*
T2 (K)	299.5 ± 2.5	299.8 ± 2.7	-0.33
925-hPa WS ($m\ s^{-1}$)	5.1 ± 3.1	4.9 ± 3.3	-0.02

5. Previously, there are also studies on the relationship between synoptic (circulation) patterns and pollution over the Beijing area, such as those cited by the authors in the introduction section. I wonder how the current study compared with these previous results. Some discussions in a general context would help.

The following discussions were added on Page 13:

"The relationship between synoptic patterns/circulations and pollution in Beijing unraveled in this study is similar to that of previous studies of Zhang et al. (2012) and Ye et al. (2016). When high pressure located to the east/southeast of Beijing, the resultant southerly PBL winds would bring the pollutants emitted from the southern Hebei to Beijing."

4

6. Figure 9 caption: "seasonally" should be "summer" because only summer data is analyzed here.

Amended as suggested.

Typos:

Page 2, line 23: in the further suppression

Page 3, line 25: the past decades

Page 4, line 5: On local scale, or "On regional scale"

Page 4, line 15: impacts on

Page5, line 25: which subjectively defines a priori … and in which the case assignment

Page 9, line 2: ...PCA which is in the S-mode …

Page 11, line 12: the lifting condensational level can drop …

Page 12, line 3: understanding the effects of …

Page 12, line 7: As illustrated in Fig. 8, …

Page 12, line 18: well captured

Page 12, line 2d: over the ENTIRE study region

Page 12, line 26: impose a negative thermal anomaly ON the PBL there

Page 13, line 5: leading to THE suppression of …

All the typos you pointed out have been revised as suggested.

References:

Abdi, H. and Williams, L. J.: Principal component analysis, Wiley Interdiscip. Rev. Comput. Stat., 2(4), 433–459, doi:10.1002/wics.101, 2010.

Bernaards, C. A. and Jennrich, R. I.: Gradient projection algorithms and software for arbitrary rotation criteria in factor analysis, Educ. Psychol. Meas., 65(5), 676–696, doi:10.1177/0013164404272507, 2005.

Richman, M. B.: Obliquely rotated principal components: An improved meteorological map typing technique?, J. Appl. Meteorol., 20(10), 1145–1159, doi:10.1175/1520-0450(1981)020<1145:ORPCAI>2.0.CO;2, 1981.

Ye, X., Song, Y., Cai, X., and Zhang, H.: Study on the synoptic flow patterns and boundary layer process of the severe haze events over the North China Plain in January 2013, Atmos. Environ., 124(January 2013), 129–145, doi:10.1016/j.atmosenv.2015.06.011, 2016.

Zhang, J. P., Zhu, T., Zhang, Q. H., Li, C. C., Shu, H. L., Ying, Y., Dai, Z. P., Wang, X., Liu, X. Y., Liang, A. M., Shen, H. X., and Yi, B. Q.: The impact of circulation patterns on regional transport pathways and air quality over Beijing and its surroundings, Atmos. Chem. Phys., 12(11), 5031–5053, doi:10.5194/acp-12-5031-2012, 2012.

6

Reviewer #2

This study utilizes four-year sounding measurements, surface PM measurements and reanalysis data to examine the influence of the synoptic patterns on the planetary boundary layer (PBL) structure and air pollution in Beijing. As Beijing has been experiencing extremely severe particulate pollution in the past few years, this study shed light on the contribution of the regional scale dynamics to the haze formation in a quantitative way. Using a synoptic pattern classification method, three patterns are identified to be closely related with heavy pollution condition in Beijing and the underlying dynamical processes are revealed in details. The cloud influence on PBL is also assessed. Overall, the manuscript is well written and I recommend publishing this study on ACP after some minor questions below can be addressed by the authors.

We thank reviewer #2 for his/her positive comments on our manuscript. In response to his/her comments, we have made relevant revisions to the manuscript. Listed below are our responses and the corresponding changes made to the manuscript according to suggestions given by the reviewer. Each comment (in black) is listed, followed by our responses (in blue).

1. Page 3, Line 9-19. I am kind of surprised that the contribution from the automobile exhaust to the Beijing air pollution was not even mentioned. Some associated references can be added here (Zhang et al., 2015, Chem. Rev.; Peng et al., 2016, PNAS)

Per your kind suggestions, the literatures concerning the contribution from automobile exhaust were added as below:

"*The major sources of aerosol in Beijing include traffic emission, power plant, industry, domestic emission, and agricultural activities (R. Zhang et al., 2015; Liu et al., 2016; Peng et al., 2016).*"

2. Page 4, Line 19. Please be specific on how the sea-breeze affects PBL and if it alleviates or deteriorates air pollution.

7

The impacts of sea-breeze on PBL structure and air pollution were added on Page 4 in the revised manuscript, as shown below.

"The diurnal variation of land-breeze and sea-breeze provides a mechanism for the pollutants in the Beijing-Tianjin-Hebei region to be recirculated and accumulated. In the evening and early morning, the presence of land-breeze (offshore wind) could bring the pollutants emitted from coastal regions to Bohai sea, and then in the afternoon, the development of sea-breeze (onshore wind) could bring these pollutants back to coastal regions, leading to exacerbated pollution. With the sea-breeze penetrates further inland, the pollutants emitted from coastal regions could be transported to the downstream regions."

3. Page 10, Line 11. I don't understand how come R is low as -0.37 but p-value is less than 0.01. What significance test is performed here?

The Pearson correlation coefficient (R) measures the linear relationship between two dataset. The closer to 1 the more 'confident' we are of a positive linear correlation and the closer to -1 the more 'confident' we are of a negative linear correlation.

The confidence in a correlation is formally determined not just by the correlation coefficient but also by the number of pairs in your data. If there are very few pairs then R needs to be very close to 1 or -1 for it to be deemed 'statistically significant', but if there are many pairs then a R closer to 0 can still considered 'highly significant' (Fenton and Neil., 2012). The critical values of R could be found at following website (Table B.7): onlinelibrary.wiley.com/doi/10.1002/9781118342978.app2/pdf

One of the standard methods to measure the 'significance' is the p-value, which is a number between 0 and 1 representing the probability that the data would have arisen if the null hypothesis (i.e., the slope of the regression line is zero) were true. In this study, there are 282 pairs of data whose correlation coefficient is -0.37, and the p-value is less than 0.01. This means the chance that we would have seen these data pairs were unrelated is less than 1%.

In this study, the p-value was calculated based on the student's t-distribution (Weathington et al., 2012), which was added in the caption of Figure 4.

4. Section 3.2. Does a haze event have to be tied to a synoptic pattern? How about a 'no wind' condition? It seems not belonging to none of the seven synoptic patterns listed there, but it did occur during some severe haze event.

Yes, every haze event develops under a specific synoptic condition, even for those haze episodes under "no wind" condition. Table S1 (in the Supplementary Materials) shows the synoptic type for each day of time period (2011 to 2014) investigated. A large body of literatures (e.g., Chen et al., 2008; Wei et al., 2011; Zhang et al., 2012) has demonstrated that a synoptic pattern is an important factor modulating the day-to-day variation of air quality. Also, the near-surface calm wind situations are often linked to a certain synoptic forcing (Kim Oanh and Leelasakultum, 2011; Ye et al., 2016), although the impacts of synoptic pattern on calm wind situations may be relatively weak, which still cannot be ignored.

5. Fig. 13. The schematic diagram is very interesting, but the mechanism only works for daytime. The pollution is typically even worse during the nighttime. It will be interesting to have some discussion about the possible PBL-synoptic pattern interactions during the nighttime.

We totally agree with the reviewer, the nocturnal boundary layer (NBL) structures/processes also play an important role in modulating the air pollution. During a diurnal cycle, the relatively high nighttime concentration of pollutants is primarily induced by the drop of BLH after sunset and the variation of emission. Besides, the daytime PBL processes also partition the pollutants within NBL and those retained in the residual layer aloft. Therefore, the following discussion has been added in the Conclusions.

"*Although this study focuses on the daytime PBL structure, the nocturnal PBL also significantly affects the air quality at hourly to diurnal scales through the intermittent turbulence, which also cannot be ignored. The structure of nocturnal PBL*

9

is primarily determined by (stull, 1988; Salmond and Mckendry, 2005). The nocturnal PBL may range from fully turbulent to intermittently turbulent or even non-turbulent at a variety of heights, temporal scales and spatial locations, which was largely induced by complex interactions between the static stability of the atmosphere and those processes (i.e. wind shear from synoptic patterns, terrain induced flows, low-level jets) that govern mechanical generation of turbulence. This makes it very difficult for the observation of large-scale atmospheric advection, investigation of the PBL-synoptic pattern interaction, transport pathways and dispersion of pollutants in the NBL, particular in regions of complex terrain such as Beijing. To fully understand the impacts of PBL on air quality in Beijing, more attention should be paid to the nocturnal PBL in the future."

References:

Chen, Z. H., Cheng, S. Y., Li, J. B., Guo, X. R., Wang, W. H. and Chen, D. S.: Relationship between atmospheric pollution processes and synoptic pressure patterns in northern China, Atmos. Environ., 42(24), 6078–6087, doi:10.1016/j.atmosenv.2008.03.043, 2008.

Fenton, N. and Neil M.: Risk Assessment and Decision Analysis with Bayesian Networks. CRC Press, 2012.

Liu, Z., Wang, Y., Hu, B., Ji, D., Zhang, J., Wu, F., Wan, X. and Wang, Y.: Source appointment of fine particle number and volume concentration during severe haze pollution in Beijing in January 2013, Environ. Sci. Pollut. Res., 23(7), 6845–6860, doi:10.1007/s11356-015-5868-6, 2016.

Kim Oanh, N. T. and Leelasakultum, K.: Analysis of meteorology and emission in haze episode prevalence over mountain-bounded region for early warning, Sci. Total Environ., 409(11), 2261–2271, doi:10.1016/j.scitotenv.2011.02.022, 2011.

Peng, J., Hu, M., Guo, S., Du, Z., Zheng, J., Shang, D., Levy Zamora, M., Zeng, L., Shao, M., Wu, Y.-S., Zheng, J., Wang, Y., Glen, C. R., Collins, D. R., Molina, M. J. and Zhang, R.: Markedly enhanced absorption and direct radiative forcing of black carbon under polluted urban environments, Proc. Natl. Acad. Sci., 113(16), 4266–4271, doi:10.1073/pnas.1602310113, 2016.

Weathington, B. L., Cunningham, C. J. L, and Pittenger, D. J.: Understanding Business Research. John Willey & Sons, 2012.

Wei, P., Cheng, S., Li, J. and Su, F.: Impact of boundary-layer anticyclonic weather system on regional air quality, Atmos. Environ., 45(14), 2453–2463, doi:10.1016/j.atmosenv.2011.01.045, 2011.

Ye, X., Song, Y., Cai, X., and Zhang, H.: Study on the synoptic flow patterns and boundary layer process of the severe haze events over the North China Plain in January 2013, Atmos. Environ., 124, 129–145, doi:10.1016/j.atmosenv.2015.06.011, 2016.

Zhang, J. P., Zhu, T., Zhang, Q. H., Li, C. C., Shu, H. L., Ying, Y., Dai, Z. P., Wang, X., Liu, X. Y., Liang, A. M., Shen, H. X., and Yi, B. Q.: The impact of circulation patterns on regional transport pathways and air quality over Beijing and its surroundings, Atmos. Chem. Phys., 12(11), 5031–5053, doi:10.5194/acp-12-5031-2012, 2012.

Zhang, R., Wang, G., Guo, S., Zamora, M. L., Ying, Q., Lin, Y., Wang, W., Hu, M. and Wang, Y.: Formation of Urban Fine Particulate Matter, Chem. Rev., 115(10), 3803–3855, doi:10.1021/acs.chemrev.5b00067, 2015.

11

Reviewer #3

It is well known that air pollution is directly associated with atmospheric boundary layer height (BLH). The daytime convective boundary layer (CBL) develops in the synoptic background. Thus the synoptic conditions affect the BLH and consequently air pollution. In this paper, the authors divided the summertime synoptic conditions in Beijing area into seven typical patterns and analyzed the BLH and air pollution level in different synoptic patterns. The results suggest that, the positive synoptic conditions promote CBL development, and higher BLH leads to light air pollution, whereas the adverse synoptic conditions suppress CBL development, and lower BLH leads to heavy air pollution. The authors provided some details about how the special synoptic conditions influence the BLH, and proposed a possible mechanism to explain the reason. The results in this paper can help to understand the impact of synoptic conditions on air pollution. However, some statements and discussion are not convincing, and the English writing should be further improved. Therefore, my recommendation is publication in ACP after major revisions.

First of all, we appreciate the reviewer's comments and suggestions. In response to the reviewer's comments, we have made thorough revisions to the manuscript. Listed below are our responses and the corresponding changes made to the manuscript according to suggestions given by the reviewer. Each comment (in black) is listed, followed by our responses (in blue).

Specific Comments

1. For Eq. (1), presence of u^* in the right hand side is an error. If the authors used this formula to calculate the BLH, the results are incorrect.

This was a typo for Eq. (1), which has been corrected in the revised manuscript.

2. This study emphasizes that heavy air pollution is caused by low BLH. But the authors did not provide solid evidences. In Fig. 3b, the results show that the diurnal variation of 1 h-bin averaged PM2.5 concentration is not significant, but the difference in BLH between 14:00 and 08:00 (or 20:00) is very larger. In addition, even for the situation at 14:00, Fig. 4b shows that the correlation coefficient between PM2.5 concentration and BLH is relatively low. Then the problem arises. What is the major reason for

12

the formation of heavy air pollution in Beijing in summertime, reduction of BLH or transportation of pollutant? In my opinion, discussing the impact of BLH on air pollution level is based on the premise that the air pollution is caused by local emissions. The above mentioned results suggest it may be not the case. If the air pollution is caused by transportation of pollutant, the low BLH may be the result

5   rather than the reason of heavy air pollution. Therefore, the authors should be cautious when discussing the relationship between BLH and air pollution level, and state their results more reasonably.

We totally agree with the reviewer, the BLH is just one of the meteorological factors modulating aerosol pollution. In the revised manuscript, the relationships between BLH and aerosol pollution were rewritten to make the explanation more reasonably. In addition, either horizontal transport of pollutants

10 or aerosol-PBL feedback plays important roles in modulating the air quality under different synoptic conditions. Therefore, the relevant discussions were added on Page 13 and Page 17 in the revised manuscript.

3.1 For the results in Fig. 8, I do not know how the authors obtained the correlation coefficients. This

15 figure shows that the correlation coefficient between PM2.5 concentration and BLH is -0.97 (the absolute value is very close to 1.0). In page 12 line 7, the authors said 'the BLH is the most crucial factor related to aerosol pollution level under different synoptic conditions'. But Fig. 4b shows that the correlation coefficient is very low (the absolute value is smaller than 0.4). I cannot understand such a large difference between the two results. The authors should explain why.

20 The correlation coefficients in Fig.8 were calculated based on the mean values for each synoptic type. For example, the correlation of BLH and $PM_{2.5}$ concentration was calculated using the seven pairs of BLH and $PM_{2.5}$ concentration. In contrast, the correlation coefficients in Fig.4 were directly calculated using daily averaged $PM_{2.5}$ concentration and its concomitant BLH. In the revised manuscript, such information was added on the caption of Fig. 8.

25

3.2 Secondly, Fig. 8 shows a high positive correlation between PM2.5 concentration and BLH and a high negative correlation between PM2.5 concentration and CLD. These results imply that the lower BLH is highly related to the larger cloud cover. It is know that the daytime CBL is driven by surface

13

heating. The large cloud cover reduces radiation arriving the surface and then the surface sensible heat flux. This may be the reason for the lower BLH in cloudy days. But the authors only emphasize the effect of capping inversion (they propose a mechanism about this as illustrated in Fig. 13).

We totally agree with the reviewer that the effect of cloudiness cannot be ignored in modulating the BLH, which should not be de-emphasized. In addition to the cloudiness, the cool/warm advections associated with different synoptic patterns may also affect the PBL structure. In the revised manuscript, to better understand the effects of cool/warm advections on PBL structure, several idealized numerical experiments were conducted.

In the idealized experiments, the simulation region was set as the same studied region shown in Fig. 1, with a horizontal grid spacing of 0.1° (~11 km). In the vertical dimension, 48 layers were set from the surface to 100-hPa level, with 21 layers between the surface and 2 km above ground level (AGL). To isolate the effects of synoptic forcing (e.g. warm/cold advection) from cloudiness, the microphysics and cumulus schemes were turned off in the idealized simulations. Similar approaches have been used by De Wekker (2008) to investigate the suppression of BLH near a mountain, and by Pu and Dickinson (2014) to investigate the dynamics of Low-Level Jet over the Great Plains.

In the revised manuscript, the description of numerical experiments were added on Page 10 to 11. And the relevant results and discussions were added on Page 15 to 16.

3.3 Thirdly, results in this figure suggest that the wind direction plays an important role in the formation of air pollution. High air pollution level is associated with south wind, implying that the pollutants may come from the cities south of Beijing. In this situation the lower BLH may be caused by the enhanced air pollution. However, the authors' analyses give me a strong feeling that the reduced BLH leads to heavy air pollution. So my question is how to interpret the results in Fig. 8. The authors should provide us a "clear picture".

As the anti-correlated relationship illustrate in Fig. 4 and Fig. 8, the reduced BLH may be one factor modulating the pollution level, however, the horizontal transport of pollutants should not be de-emphasized as the reviewer suggested. In the revised manuscript, we try to provide a more "clear picture" about the relationships between meteorological factors/processes (i.e., BLH, horizontal

14

transportation, aerosol-PBL feedback) and pollution. The relevant discussions were added on Page 13 to 14.

4. Page 13, line 1-2 'Among the seven identified synoptic patterns, the strongest near-surface could advection is associated with Type 1 (Fig. 11a), leading to the coldest PBL at 1400 BJT (Fig. 9a)', and line 5-6 'Types 2, 4, 5 and 6 also show cold advection toward Beijing but it is less prominent (Figs. 11b and 11d-f)'. I am not sure if the PT anomaly is caused by cold advection. Large cloud cover may also reduce PT in the boundary layer. The PT anomaly in Type 2 is similar to that in Type 1, and the other conditions in the two types are almost the same: the same CLD, no warm advection above CBL top. Why Type 1 has a negative BLH anomaly but Type 2 has a positive BLH anomaly? Moreover, the BLH in Type 1 is slightly lower than the seasonal average while the BLH in Type 2 is slightly higher than the seasonal average (as shown in Fig. 6a), and the BLH difference in the two types is merely about 200 m. Why such a small difference in BLH can introduce large difference in $PM_{2.5}$ concentration (one is 101 μg m-3, another is 67μg m-3)? I guess, transportation of high concentration pollutants may contribute to heavy air pollution in Type1, because Type 1 has south wind whereas Type 2 has east wind.

We agree with the reviewer, the large difference of $PM_{2.5}$ concentration between Type 1 and Type 2 may be primarily caused by the different horizontal transport of pollutants. The relevant discussions were added on Page 13 in the revised manuscript.

Besides, to understand the impacts of cool/warm advection on PBL structure, several idealized simulations were conducted to isolate the impacts of advection from other factors, such as the cloudiness and aerosol-PBL feedback. As the simulated cross section of PT shown in Fig. 11, the cold/warm advection could play a role in modulating the PBL structure in Beijing. The relevant discussions were added on Page 15-16 in the revised manuscript.

5. For Fig. 11, I do not think the PT anomaly and the wind field can match very well. Fig. 11d shows an elevated negative PT-anomaly area, stretching from the right to the left. But the wind direction is form the left to the right together with a downward component. Actually, Fig. 6a shows that the boundary layer wind blows towards northeast (with a relatively small west component). It means that the flow

15

passing Beijing does not come from Bohai or Yellow Sea (the same evidence can be found in Fig. 10d). Also, Fig. 11e shows an isolated maximum negative PT-anomaly area over Beijing. If this negative PT-anomaly area is caused by cold advection, the magnitude of PT-anomaly in the right area should be larger than, or at least the same as, that in this area. I mean the maximum negative PT-anomaly area

5 should stretch to the right side of picture, as shown in Figs. 11a&b or Fig. 11f. Can the isolated maximum negative PT-anomaly area over land be regarded as the result of cold advection from sea? In my opinion, the isolated maximum negative PT-anomaly area over Beijing implies a local cooling. So, my question is, can the negative PT-anomaly be interpreted as the result of cold advection from sea? I think the authors should discuss this issue cautiously.

10   We agree with the reviewer, the development of PBL can be extremely complex, influencing by the cloudiness, warm/cold advection, and aerosols at the same time. And the resolution of FNL reanalysis may be not enough to study the PBL structure/process. Thus, in the revised manuscript, seven idealized numerical experiments were conducted to understand the effects of cold/warm advection on PBL structure, in which the effects of cloudiness were isolated through turning off relevant

15 parameterization schemes. The relevant discussions were added on Page 15-16 in the revised manuscript.

6. For Fig. 13, I suggest to remove this schematic map. I think there is no solid evidence to support the so-called "advection mechanism". The authors can add the seasonal mean PT profile in each panel of

20 Fig. 9. By comparing the PT profile in each type with the seasonal mean PT profile, we can know whether the capping inversion is enhanced or weakened in each synoptic pattern. Then the authors can discuss the possible reasons.

     The schematic diagram was removed as suggested, and the revised Fig.9 was drawn, in which the PT anomaly (subtracted from the seasonally averaged PT profile in summer) for each synoptic type

25 was added.

     For Types 1, 4, and 5, the differential cooling/ warming anomalies within PBL and above it play a role in enhancing the thermal inversion at PBL top, which would suppress the development of PBL. Specifically, the cooling (warming) of Type 1 (4) is stronger (weaker) within PBL than that above it;

16

and for Type 5, the PT anomaly within PBL is negative while that above PBL is positive. In contrast, the PT anomaly of other Types (2, 3, 6, and 7) tend to lower the thermal inversion at PBL top to some extent, favoring the growth of PBL. These PT anomalies and resultant BLHs could be partially responsible to the different pollution level for different synoptic types. In the revised manuscript, the
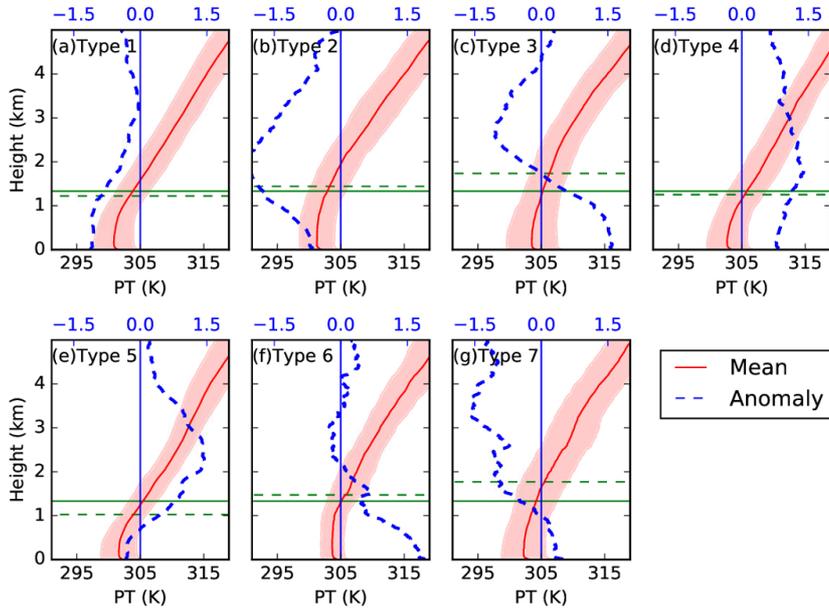
5   relevant discussions were added on Page 15.

Fig. 9. Vertical profiles of potential temperature (PT) at 1400 BJT associated with the seven types of synoptic pattern derived from soundings (red lines). Solid lines indicate average values and shaded

10   *areas show the uncertainty range (the mean ± one standard deviation). Green solid lines represent the summer averaged BLH and green dashed lines represent the average BLH for each synoptic type. The PT anomaly (subtracted from the summer averaged PT profile) for each synoptic type was also given by the blue dash-lines in each panel.*

17

7. For the English wording and writing, I suggest that the authors get a fluent writer/speaker of English to look through the paper.

Per your kind suggestion, a native speaker has been invited to review the manuscript.

5

References:

De Wekker, S. F. J.: Observational and numerical evidence of depressed convective boundary layer heights near a mountain base, J. Appl. Meteorol. Climatol., 47(4), 1017–1026, doi:10.1175/2007JAMC1651.1, 2008.

10 Pu, B. and Dickinson, R. E.: Diurnal spatial variability of Great Plains summer precipitation related to the dynamics of the low-level jet, J. Atmos. Sci., 71, 1807–1817, doi:10.1175/JAS-D-13-0243.1, 2014.

18

Classification of summertime synoptic patterns in Beijing and their associations with boundary layer structure affecting aerosol pollution

Yucong Miao[1], Jianping Guo[1], Shuhua Liu[2], Huan Liu, Zhanqing Li[3, 4], Wanchun Zhang[1], and Panmao Zhai[1]

[1]State Key Laboratory of Severe Weather & Key Laboratory of Atmospheric Chemistry of CMA, Chinese Academy of Meteorological Sciences, Beijing 100081, China

[2]Department of Atmospheric and Oceanic Sciences, Peking University, Beijing 100871, China

[3]College of Global Change and Earth System Science, Beijing Normal University, Beijing 100875, China

[4]Dept. of Atmospheric & Oceanic Sciences and ESSIC, University of Maryland, College Park, MD 20740, USA

Correspondence to: Jianping Guo, PhD/Prof. (jpguocams@gmail.com)
             Zhanqing Li, PhD/Prof. (zli@umd.edu)

19

Abstract

Meteorological conditions within the planetary boundary layer (PBL) are closely governed by large-scale synoptic patterns and play important roles in air quality by directly and indirectly affecting the emission, transport, formation, and deposition of air pollutants. Partly due to the lack of long-term fine-resolution observations of the PBL, the relationships between synoptic patterns, PBL structure, and aerosol pollution in Beijing have not been well understood. This study applied the obliquely rotated principal component analysis in T-mode to classify the summertime synoptic conditions over Beijing using the National Centers for Environmental Prediction reanalysis from 2011 to 2014, and investigated their relationships with PBL structure and aerosol pollution by combining numerical simulations, measurements of surface meteorological variables, fine-resolution soundings, the concentration of particles with diameters less than or equal to 2.5 μm, total cloud cover (CLD), and reanalysis data. Among the seven identified synoptic patterns, three types accounted for 67% of the total number of cases studied and were associated with heavy aerosol pollution events. These particular synoptic patterns were characterized by high-pressure systems located to the east or southeast of Beijing at the 925-hPa level, which blocked the air flow seaward, and southerly PBL winds that brought in polluted air from the southern industrial zone. The horizontal transport of pollutants induced by the synoptic forcings may be the most important factor affecting the air quality of Beijing in summer. In the vertical dimension, these three synoptic patterns featured a relatively low boundary layer height (BLH) in the afternoon, accompanied by high CLD and southerly cold advection from the seas within the PBL. The high CLD reduced the solar radiation reaching surface, and suppressed the thermal turbulence, leading to lower BLH. Besides, the numerical sensitive experiments show that cold advection induced by the large-scale synoptic forcing may have cooled the PBL, leading to an increase in near-surface stability and a decrease in the BLH in the afternoon. Moreover, when warm advection appeared simultaneously above the top level of the PBL, the thermal inversion layer capping the PBL may have been strengthened, resulting in the further suppression of PBL and thus the deterioration of aerosol pollution levels. This study has important implications for understanding the crucial roles that meteorological factors (at both synoptic and local scales) play in modulating and forecasting aerosol pollution in Beijing and its surrounding area.

20

1 Introduction

Beijing, located on the North China Plain (Fig. 1), is the center of politics, culture, and economics in China. With its rapid urbanization, tremendous economic development, and concomitant increase in energy usage, heavy air pollution episodes largely caused by high aerosol loading have been frequently reported in Beijing (Chan and Yao, 2008; Guo et al., 2011; Guo et al., 2013; San Martini et al., 2015; Zhang and Cao, 2015). Great efforts, therefore, have been devoted to investigating air quality issues in Beijing through comprehensive observational and modelling studies (He et al., 2001; Zhu et al., 2011; Liu et al., 2013; Quan et al., 2013; Zhang et al., 2013; Guo et al., 2014; Wang et al., 2015a; Z. Zhang et al., 2015; Ye et al., 2016). The major sources of aerosol in Beijing include traffic emission, power plant, industry, domestic emission, and agricultural activities (R. Zhang et al., 2015; Liu et al., 2016; Peng et al., 2016). In an annual cycle, the aerosol pollution in Beijing has different characteristics in different seasons. In spring, the majority of heavy aerosol pollution is associated with dust storms (He et al., 2001; Zhao et al., 2007; Guo et al., 2013). During summer and fall, photochemical production and agricultural burning may play a role in exacerbating the air quality (Zhang et al., 2013; Wang et al., 2015b). In winter, frequent severe haze events were found to be associated with the substantial increase in coal combustion for heating (Zhang et al., 2013; Tang et al., 2015). Air quality can be further deteriorated through secondary aerosol formation (e.g., Huang et al., 2014; Han et al., 2015).

In addition to high emissions and aerosol chemistry processes, meteorological conditions also play important roles in the formation and evolution of aerosol pollution in Beijing (Zhang et al., 2012; Quan et al., 2013; Hu et al., 2014; Miao et al., 2015b; Ye et al., 2016; Z. Zhang et al., 2015). In the heavily populated monsoon region (e.g., Beijing), the large-scale distributions and variations of aerosol loading are strongly influenced by the monsoon circulations (Zhang et al., 2010; Li et al, 2016; Wu et al., 2016), since the monsoon circulations directly determine the large-scale transport and lifetime of aerosols. In addition to the increase of anthropogenic emissions during the past decades in China, the recently frequent occurrence of aerosol pollution in China has been found to be associated with the variability in Monsoon (Niu et al., 2010; Zhang et al., 2010; Liu et al., 2011).

On regional scale, detailed statistical analyses have also shown that heavy aerosol pollution in Beijing is associated with southerly winds, high relative humidity (RH), stable atmospheric

21

stratification, and a low boundary layer height (BLH) (Quan et al., 2013; H. Zhang et al., 2015; Tang et al., 2016; Ye et al., 2016). Among these local meteorological factors, the BLH is one of the most crucial factors because it directly determines the total dispersion volume (Quan et al., 2013; Hu et al., 2014; Tang et al., 2016) and has a strong influence on the occurrence, maintenance, and dissipation of aerosol

5 pollution in Beijing (e.g., Miao et al., 2015b).

With the Yan and Taihang Mountains to the north and west of Beijing (Fig. 1), the thermally-induced mountain-plain breeze circulation can be well developed under favorable synoptic conditions, which impacts on the PBL structure and modulates aerosol pollution (De Wekker, 2008; Chen et al., 2009; Liu et al., 2009; Hu et al., 2014; Miao et al., 2015b, 2016). Since the Bohai Sea is located ~150

10 km to the southeast of China (Fig. 1), a sea-breeze (Miller, 2003) can be established and penetrate inland to Beijing. This can also play a role in affecting the PBL structure and air quality (Liu et al., 2009; Sun et al., 2013; Miao et al., 2015a, 2015b). The diurnal variation of land-breeze and sea-breeze provides a mechanism for the pollutants in the Beijing-Tianjin-Hebei region to be recirculated and accumulated; in the evening and early morning, the presence of land-breeze (offshore wind) could bring

15 the pollutants emitted from coastal regions to Bohai sea, and then in the afternoon, the development of sea-breeze (onshore wind) could bring these pollutants back to coastal regions, leading to exacerbate pollution. With the sea-breeze penetrates further inland, the pollutants emitted from coastal regions could be transported to the downstream regions.

Although the importance of the PBL structure on air pollution has been widely recognized (Wang et

20 al., 2014; Miao et al., 2015b; Tang et al., 2016), more investigations are warranted concerning (1) the crucial factors affecting the development of the PBL and (2) the relationships between large-scale synoptic forcing and the structure of the PBL. They are yet to be fully understood, partly due to the lack of long-term fine-resolution PBL observations (Liu and Liang, 2010). Radiosondes are conventionally launched twice a day at 0000 (0800) and 1200 (2000) Coordinated Universal Time (UTC) (Beijing

25 Local Time, BJT). Most data are only reported at significant pressure levels with at most six records below 500-hPa (Liu and Liang, 2010), which cannot capture the fine structure of the PBL.

22

已删除: Stull, 1988;

已删除: the structure of the planetary boundary layer (PBL). The latter

已删除: ; Ding et al., 2016; Petäjä et al., 2016; Tang et al., 2016)

已设置格式: 字体颜色: 自动

已删除: s

In 2011, an L-band radiosonde network across China (Guo et al., 2016; Zhang et al., 2016) was established by the China Meteorological Administration. This network of measurements provides fine-resolution profiles of temperature (Fig. 2), pressure, RH, and wind speed and direction twice a day (0800 and 2000 BJT). Additional soundings are made at 1400 BJT in the summertime (June-July-

5   August, the wet season) at the Beijing site (39.80°N, 116.47°E) (the blue cross in Fig. 1). These fine-resolution sounding observations allow for the investigation of the PBL structure over Beijing.

The development of the PBL is mainly controlled by large-scale external synoptic conditions and by local surface sensible heat fluxes (Garratt, 1994). So in this study, not only are local factors that affect the surface heat budget analyzed (e.g., cloud cover), but also the large-scale synoptic forcing. A

10   synoptic regime is defined by large-scale warm/cold advection and transport pathways of water vapor and pollutants (Zhang et al., 2012; Zhao et al., 2013; Ye et al., 2016), which can affect the PBL structure and air quality (Miao et al., 2015b; Ye et al., 2016). The variation of the synoptic patterns modulated the ambient pollutants and likely provided the primary driving force for the day-to-day variations in air pollution level (e.g., Chen et al., 2008; Wei et al., 2011; Zhang et al., 2012; Hu et al.,

15   2014; Ding et al., 2016). Besides, severe aerosol pollution events in Beijing tend to occur more frequently under stable and weak anticyclone synoptic conditions (e.g., Zhang et al., 2012; Liu et al., 2013; Li et al., 2015). However, most previous studies evaluated the impacts of synoptic types through case studies for short periods (Chen et al., 2009; Hu et al., 2014; Quan et al., 2014; Tie et al., 2015; Miao et al., 2016), which is not suitable for identifying dominant synoptic patterns.

20   In this study, we employ a climatological approach to classify the summertime synoptic patterns over Beijing from 2011 to 2014, the same objective classification approach applied by Zhang et al. (2012) and Ye et al. (2016) to classify synoptic types in the North China Plain. Zhang et al. (2012) identified nine synoptic patterns using the daily surface-level pressure fields from 2000 to 2009, and Ye et al. (2016) presented a more detailed classification of synoptic patterns for fall and winter. They found

25   that the poor air quality in Beijing was associated with high pressure to the east and a relatively low BLH. However, previous studies did not unravel the causes of the low BLH and the physical mechanisms underlying it, partly due to the lack of appropriate observational data (e.g., fine-resolution soundings in the afternoon, cloud cover). In addition, the north-south movement of the subtropical

23

已设置格式: 字体颜色: 自动

已删除: have found to
已删除: be
已删除: red
已删除: ，   ... [1]
已删除: M
已删除: .

已删除: This approach is not suitable for identifying dominant synoptic patterns. Studying large-scale synoptic patterns allows us to consider the numerous interrelated meteorological variables within an integrated framework (Zhang et al., 2012), thus providing an insight into the physical mechanisms underlying aerosol pollution in Beijing.
已删除: ，   ... [2]
已删除: T
已删除: was

anticyclone plays an important role in modulating the seasonal variation in prevailing synoptic patterns in Beijing (Miao et al., 2015b). It is thus better to classify synoptic patterns for each season.

In summer, although the aerosol pollution level in Beijing is lower than that in fall and winter (Fig. 3a), the seasonally average concentration of particles with diameters less than or equal to 2.5 μm

5 ($PM_{2.5}$) is still as high as 85.7 μg m^{-3}, based on data from 2011 to 2014. This is 2.4 times higher than the national standard level (35 μg m^{-3}). Also, the relationships between aerosol pollution, the PBL structure, and synoptic patterns in summer are rarely studied, which will be systematically evaluated using long-term observations. This study will extend previous studies as it is an attempt to understand the impacts of large-scale synoptic forcing on the PBL structure and air quality. The remainder of this paper is

10 organized as follows. In section 2, the methodology and data are described. In section 3, the summertime synoptic types are classified, and their relationships to aerosol pollution and the PBL structure are investigated. The main findings are summarized in section 4.

2 Data and methods

15 2.1 Data

To classify the summertime synoptic types in Beijing, geopotential height (GH) fields derived from the National Centre for Environmental Prediction (NCEP) global Final (FNL) reanalysis (http://rda.ucar.edu/datasets/ds083.2/) from 2011 to 2014 are used. The NCEP-FNL reanalysis is produced by the Global Data Assimilation System, which continuously assimilates observations from

20 the Global Telecommunication System and other sources. The NCEP-FNL reanalysis fields are on 1° × 1° grids with a 6-hour temporal resolution, i.e., 0000 (0800), 0600 (1400), 1200 (2000), and 2000 (0200) UTC (BJT).

In this study, daily GH fields at the 925-hPa level from the NCEP-FNL reanalysis covering the Beijing-Tianjin-Hebei (BTH) region (43°N-47°N, 112°E-125°E) (Fig. 1) were classified to identify the

25 prevailing synoptic types in summer. Results from the classification of the 925-hPa GH field are similar to those using the GH fields at other tropospheric levels because there is a high degree of dependence among individual levels (Huth et al., 2008).

24

To investigate the PBL structures associated with different synoptic types, summertime soundings collected at the Beijing site (39.80°N, 116.47°E) for the period 2011-2014 were analyzed. This sounding station, equipped with an L-band radiosonde system (Guo et al., 2016), provides atmospheric sounding data (profiles of temperature, RH, wind speed and direction) up to three times a day (0800, 1400, and 2000 BJT) at a high vertical resolution. In total, 1055 effective soundings were obtained for this study: 357 soundings at 0800 BJT, 332 soundings at 1400 BJT, and 366 soundings at 2000 BJT. In addition, the total cloud cover (CLD) was observed four times a day (0200, 0800, 1400, and 2000 BJT) and hourly near-surface observations (temperature, RH, wind speed and direction, and precipitation amount) were made.

The aerosol pollution level in Beijing is denoted by the near-surface $PM_{2.5}$ concentration. Since 2008, U.S. diplomatic missions in China have monitored $PM_{2.5}$ concentrations and have made both real-time and historic data available to the public (www.stateair.net). Hourly $PM_{2.5}$ concentrations in Beijing (the red dot in Fig. 1) are measured using a beta attenuation monitor (BAM) (Chung et al., 2001) installed on the roof of the U.S. Embassy (39.95°N, 116.47°E). The BAM technique is a reference method for measuring $PM_{2.5}$ concentrations that is used by the U.S. Environmental Protection Agency. In this study, summertime $PM_{2.5}$ concentration measurements from 2011 to 2014 were used to investigate the relationship between aerosol pollution and synoptic patterns in Beijing.

2.2 BLH derived from soundings

The bulk Richardson number (Ri) method (Vogelezang and Holtslag, 1996) was applied to estimate the BLH in Beijing from sounding data because it is suitable for both stable and convective PBLs (Seidel et al., 2012). The Ri is defined as the ratio of turbulence associated with buoyancy to the turbulence caused by mechanical shear:

$$\text{Ri}(z) = \frac{(g/\theta_{vs})(\theta_{vz} - \theta_{vs})(z - z_s)}{(u_z - u_s)^2 + (v_z - v_s)^2 + bu_*^2} \quad , \quad (1)$$

where z is the height (above ground level, AGL), g is the acceleration caused by gravity, θ_v is the virtual potential temperature, u and v are the components of the observed wind speed, b is a constant, and u_* is

25

the surface friction velocity. The subscript s denotes the surface level. Since u_* is not known from the sounding observations, and its magnitude is much smaller than that of the bulk wind shear term in the denominator (Vogelezang and Holtslag, 1996), we set b = 0 and ignore the surface frictional effect. The BLH is referred to as the lowest level z at which the interpolated Ri crosses the critical value of 0.25. A

5 similar criterion was applied to investigate PBL climatologies by Seidel et al. (2012) for the U.S. and by Guo et al. (2016) for China. A case in point for the BLH derived from the sounding profiles of θ_v and Ri at the Beijing site is shown in Fig. 2.

2.3 Classification of synoptic types

10 Approaches used to classify synoptic patterns can be roughly split into two groups: subjective and objective. The subjective approach is usually referred to as manual classification, which subjectively defines a priori and in which the case assignment is also subjective (Huth et al., 2008). A subjective classification is arbitrary to a large extent. By contrast, an objective approach defines types and assigns cases using numerical procedures based on the measures of (dis)similarity and variance maximization.

15 Because an objective classification is capable of processing large amounts of data and depends less on one's experience, we choose the objective approach (Huth et al., 2008) to identify synoptic types in Beijing. Studying large-scale synoptic patterns allows us to consider the numerous interrelated meteorological variables within an integrated framework (Zhang et al., 2012), thus providing an insight into the physical mechanisms underlying aerosol pollution in Beijing.

20 The obliquely rotated principal component analysis in T-mode (T-PCA) approach (Richman, 1981; Huth et al., 2008) was first used to analyze large-scale synoptic conditions through classification of the predominant synoptic types, which was adopted for air quality studies (e.g., Stefan et al., 2010; Zhang et al., 2012). The T-PCA calculates the eigenvectors of the input data set by singular value decomposition and finds typical patterns by loadings that can be divided into classes. The application of

25 the PCA in T-mode means that daily patterns form the columns in the input data matrix and grid-point values form its rows (Huth, 2000). Unlike the common application of PCA in the S-mode, which is used to isolate subgroups of grid points that co-vary similarly, the T-PCA is used to isolate subgroups of similar spatial patterns. This approach has proven to be a reliable classification method, largely due to

26

已删除: which is

its temporal and spatial stability, in addition to its ability to reproduce predefined dominant patterns with little dependence on pre-set parameters (Huth, 1996; Philipp et al., 2010).

In this study, the T-PCA classification based on Huth (2000) was done using the cost733class software package (http://cost733.met.no), which was developed for creating, comparing, and evaluating classifications in several variants. To speed up the calculation of PCA, the data is split into ten subsets; and then, the principle components (PCs) obtained from each subset are projected on the rest data. The T-PCA classification based on cost733 software package includes the following steps:

(1) The data is standardized spatially. Each pattern's mean is subtracted from the data, and then the patterns are divided by their standard deviations.

(2) The data is split into ten subsets through selecting the data once every ten days. For example, the first subset consists of the 1st, 11th, 21st, 31st, etc. days, and the second subset consists of the 2nd, 12th, 22nd, 32nd, etc. days.

(3) The PCs are calculated using the singular value decomposition for each subset. And the PCs of each subset are ordered according to the magnitude of their explained variances.

(4) An oblique rotation (using direct oblimin) is applied on the PCs, employing an adaptation of the Gradient Projection Algorithm of Bernaards and Jennrich (2005). The main reason for using rotation is to facilitate the interpretation (Abdi and Williams, 2010). This transformation does not constrain the orthogonality, allowing for the PCs the freedom to better reflect the original data (Richman, 1981).

(5) The PC scores of each subset are projected onto the remaining data by solving the matrix equation: $\Phi A^T = F^T Z$, where F and Φ are matrices of PC scores and PC correlations, respectively, and Z is the full data matrix, and A are pseudo-loadings to be determined. Each day is classified with the PC (type) for which it has the highest loading.

(6) Contingency tables are finally used to compare the ten classifications, and the classification most consistent with the other nine classifications is selected as the resultant one.

Using the T-PCA module of the cost733class software package to classify synoptic types, the number of PCs needs to be explicitly defined. To understand the relationships between synoptic types,

PBL structures, and aerosol pollution, we tested the classification using different numbers of principal components (e.g., 4, 5, 6, 7, 8, 9), and compared the results with the observed BLH and $PM_{2.5}$ concentration (Fig. S1). The classification using seven principal components shows the most significant anti-correlation between BLH and $PM_{2.5}$ concentration (R = -0.97, p < 0.01, Fig. S1). This will be discussed further in section 3.

2.4 Idealized numerical experiments

Considering the PBL structure being simultaneously modulated by the cloudiness, warm/cold advection, and aerosols, to better understand the relationships between the synoptic condition and PBL structure in Beijing, the Weather Research and Forecasting model (WRF version 3.7.1) was used to conduct seven idealized numerical experiments: each corresponds to one of the seven identified synoptic patterns.

In the idealized experiments, the simulation region was set as the same studied region shown in Fig. 1, with a horizontal grid spacing of 0.1° (~11 km). In the vertical dimension, 48 layers were set from the surface to 100-hPa level, with 21 layers between the surface and 2 km above ground level (AGL). To isolate the effects of synoptic forcing (e.g. warm/cold advection) from cloudiness, the microphysics and cumulus schemes were turned off in the idealized simulations. Similar approaches have been used by De Wekker (2008) to investigate the suppression of BLH near a mountain, and by Pu and Dickinson (2014) to investigate the dynamics of Low-Level Jet over the Great Plains. The other physics parameterization schemes utilized by this study included the Yonsei University (YSU) PBL scheme (Hong et al., 2006), the updated rapid radiative radiation scheme (Iacono et al., 2008), and the Noah land surface scheme (Chen and Dudhia, 2001) with a single-layer urban canopy model (Kusaka et al., 2001).

For the initial and boundary conditions (IBCs) of humidity and temperature for the atmosphere, ocean, and soil, all the seven idealized simulations were set up using the summertime seasonal means derived from the NCEP-FNL reanalysis from 2011 to 2014. And the IBCs of wind and pressure were set up using the means of each synoptic pattern obtained from the NCEP-FNL reanalysis. All these

28

boundary conditions were cycled periodically in time, i.e., from 000 to 0600 to 1200 to 1800 UTC, and then back to 0000 UTC. To represent the seasonal mean solar radiation forcing in summer, all these seven simulations were initialized at 0800 BJT (0000 UTC) 14 July. The simulations were run for 42 hours, and the first 30 hours were considered as the spin-up period. Such numerical configurations allowed us to examine the influences of different synoptic forcing on PBL structure in Beijing, isolating from the effects of cloudiness.

3 Results and discussion

3.1 Relationships between the BLH and aerosol pollution in summer

During a diurnal cycle, the development of the PBL is closely tied to solar heating of the ground (Stull, 1988). After sunrise, the PBL in Beijing during summer undergoes a transition from a nocturnal stable PBL to a convective PBL, and reaches its maximum depth in the afternoon (c.f., Fig. 3b), remaining there until sunset (Stull, 1988). After sunset, without sufficient heat fluxes to maintain the convective PBL, the BLH drops quickly (Fig. 3b). Along with the diurnal evolution of the BLH, the near-surface $PM_{2.5}$ concentration exhibits a nearly reversed diurnal variation. The $PM_{2.5}$ concentration is generally low in the afternoon and reaches its peak values in the evening and early morning.

As shown in Fig. 4, the BLHs derived from soundings were compared with their corresponding daily average $PM_{2.5}$ concentrations. At 0800 BJT, the PBL is typically shallow and its depth is statistically uncorrelated with the daily $PM_{2.5}$ concentration (R = -0.03, p = 0.62, Fig. 4a). At 1400 BJT, the PBL is fully developed, with an average BLH of ~1.3 km, which is clearly anti-correlated with the daily $PM_{2.5}$ concentration (R = -0.36, p < 0.01, Fig. 4b). This implies that the variation in afternoon BLH plays an important role in modulating the day-to-day variation of aerosol pollution level in Beijing. At 2000 BJT, the PBL is in transition from a convective state to a nocturnal stable state, and the BLH becomes uncorrelated with the daily $PM_{2.5}$ concentration (R = 0.10, p = 0.09, Fig. 4c). Averaged over the whole day, a significantly negative correlation (R = -0.32, p < 0.01) is still found between the daily BLH and $PM_{2.5}$ concentration (Fig. 4d). When excluding observations made on rainy days, a stronger correlation (R = -0.37, p < 0.01) is obtained. So in this study, we mainly investigate the factors that determine the BLH at 1400 BJT and their relationships with large-scale synoptic patterns.

3.2 Synoptic patterns and aerosol pollution

Using the T-PCA classification based on the summertime 925-hPa GH field, seven dominant types of synoptic patterns (Fig. 5 and Table S1) were identified. According to the locations of high and low

5 pressure systems with respect to Beijing (Fig. 5), these seven synoptic types can be briefly described as (1) high pressure to the east, (2) high pressure to the north, (3) low pressure to the northeast, (4) low pressure to the north, (5) low pressure to the northwest, (6) weak high pressure over Beijing, and (7) low pressure to the east.

Among these seven identified synoptic patterns, Types 1, 4, and 5 are associated with heavier

10 aerosol pollution (Fig. 5), all with an average $PM_{2.5}$ concentration greater than 90 μg m^{-3}. These three types are also the most frequent synoptic patterns in summer, accounting for 67% of the total. At the 925-hPa level, the three synoptic patterns are characterized by a high pressure system located to the east or southeast of Beijing, which brings southerly winds to Beijing, but blocks the polluted air from moving away eastwards towards the Yellow Sea (Figs. 5 and S2). Southerly winds are not only

15 observed at the 925-hPa level, but also throughout almost all of the PBL (Fig. 6a). With the southerly PBL winds blowing over the plains of the BTH region, pollutants emitted from the surrounding southern cities (e.g., Baoding, Shijiazhuang, and Cangzhou) can be transported to Beijing (Wang et al., 2010; Zhang et al., 2012; Miao et al., 2016), leading to a worsening of the air quality in Beijing. The impacts of synoptic forcings (i.e. high pressure to the east or southeast of Beijing and resultant southerly

20 winds) on the transport of pollutants from adjacent regions to Beijing have also been reported by Zhang et al. (2012) and Ye et al. (2016).

In addition to the southerly PBL winds, high 2-m RH (RH2), high CLD, and low BLH are other crucial parameters associated with severe aerosol pollution (Figs. 6 and 7, Table S2). At 1400 BJT, all three synoptic patterns (Types 1, 4, and 5) have a relatively low BLH (Fig. 6a, and Table S2), with an

25 average value less than 1.4 km. This would limit the vertical dispersion of pollutants to some extent, and exacerbate the pollution. Meanwhile, Types 1 and 5 are characterized by relatively high CLD and RH2 (Fig. 6b), which could facilitate the hygroscopic growth of aerosols (Kim et al., 2014; Ye et al., 2016).

30

已删除: s

已设置格式: 字体颜色: 自动

已设置格式: 字体颜色: 自动

Among all these meteorological factors/processes, the horizontal transport of pollutants driven by different synoptic patterns may be the most important factor modulating the air quality. For example, Fig. 5 reveals a large difference of $PM_{2.5}$ concentration between Type 1 (101 μg m^{-3}) and Type 2 (67μg m^{-3}), while their CLD and RH2 are quite similar, and the difference of BLH is only ~ 0.2 km (Fig. 6).
5 For these two synoptic types, the large difference of aerosol concentration could be attributed to the different horizontal transport induced by the different prevailing winds (i.e., southerly wind for Type 1 and easterly wind for Type 2). And the pollution of Type 1 may be exacerbated by the relatively low BLH in the afternoon. Besides, during the pollution episodes, the presence of aerosols within PBL may also play a role in modulating the PBL structure through portioning the solar radiation between land
10 surface and PBL (Li et al., 2007; Ding et al., 2016; Miao et al., 2016). On one hand, the presence of aerosols could reduce the solar radiation reaching land surface. The absorbing aerosols could heat the atmosphere, leading to a more stable and shallower PBL during the daytime (Quan et al., 2013; Gao et al., 2015).

Additionally, as illustrated in Figure 7, the RH2, CLD, and BLH are highly related. The increase in
15 CLD reduces the amount of solar radiation reaching the surface, and suppresses the development of the PBL and the vertical mixing of water vapor, leading to a decrease in the BLH and an increase in RH2. The high CLD could be at least partially responsible for the relative shallow PBL in the afternoon. On the other hand, when RH2 increases, the lifting condensational level (LCL) can drop, favoring the formation of cumulus clouds, which may subsequently suppress the development of the PBL (Wilde et
20 al., 1985; Craven et al., 2002; Zhu and Albrecht, 2002). As a result, under clear conditions (CLD < 20%), the average RH2 is less than 40% while the average BLH at 1400 BJT can reach ~2.2 km (Fig. 7), favoring the vertical dispersion of aerosols. By contrast, under cloudy conditions (CLD > 80%), the average RH2 and BLH increases to ~70% and decreases to ~1.2 km, respectively.

Figure 8 shows the correlations between average $PM_{2.5}$ concentrations and meteorological variables
25 for the different synoptic patterns. The $PM_{2.5}$ concentration in Beijing is significantly correlated with the southerly wind at the 925-hPa level, RH2, and CLD at 1400 BJT, and anti-correlated with the BLH at 1400 BJT. By contrast, the $PM_{2.5}$ concentration is uncorrelated with the 2-m temperature and wind speed. Types 1, 4, and 5 synoptic patterns associated with southerly PBL winds, high CLD, low BLH,

31

and high RH2 in Beijing favor the occurrence of heavy aerosol pollution in summer. By contrast, synoptic patterns with strong northerly PBL winds (Types 3 and 7) or relatively high BLH (Types 2 and 6) are associated with good air quality conditions in Beijing.

In addition to the aforementioned meteorological factors, precipitation may also affect aerosol pollution levels through wet scavenging (Yoo et al., 2014). Therefore, for each identified synoptic pattern, we examined the aerosol pollution after removing observations made on rainy days (Figs. S3 and S4). Similar relationships between aerosol pollution, RH2, CLD, BLH, and synoptic patterns were found, suggesting that whether it rains or not is not important when it comes to understanding effects of synoptic patterns on PBL structure and aerosol pollution in Beijing.

3.3 Large-scale synoptic warm/cold advection and PBL structures

Figure 9 shows the averaged PT profile and its anomaly (subtracted from the seasonally averaged PT profile in summer) for each synoptic type. For Types 1, 4, and 5, the differential PT anomalies within and above PBL play a role in enhancing the thermal inversion at PBL top, which would suppress the development of PBL (Figs. 9a, 9d, and 9e). Specifically, the cool (warm) anomaly of Type 1 (4) is stronger (weaker) within PBL than the upper level. And for Type 5, the PT anomaly within PBL is negative while that above PBL top is positive. In contrast, the PT anomaly of other Types (2, 3, 6, and 7) tends to weaken the thermal inversion at PBL top, which would favor the growth of PBL to some extent.

How do these different PBL thermal structures develop under different synoptic conditions? As discussed in section 3.2, the high CLD could reduce the solar radiation reaching land surface, leading to suppression of PBL during the daytime. The cloudiness may be one factor leading to the different PBL structures. In addition, the BLH of different synoptic pattern is also highly related with RH2 and southerly winds at 925-hPa level (Fig. 8). Can the different synoptic winds and resultant warm/cold advections modulate the PBL structure?

To determine the possible effects of warm/cold advection on PBL structure, the three-dimensional PT fields and wind vectors obtained from the idealized simulations were analyzed, in which the effects

32

of cloudiness were isolated. As the simulated BLH at 1400 BJT shown in Fig.10, significant differences could be noted among the simulated BLHs of different synoptic patterns. In Figure 10, the simulated BLH at 1400 BJT of each synoptic pattern is also compared with that derived from soundings. Both the simulations and observations show the same variation trend of BLH from Type 1 to Type 7, except for the relatively high BLH of Type 6 simulated by WRF. In other words, the variations of BLH among the seven synoptic patterns are well reproduced by the idealized simulations, although the simulated BLH is generally higher than the observed BLH, which may be caused by the simplification of cloud processes in the idealized simulations. With the weakest pressure gradient over Beijing (Fig. 5f), the large-scale synoptic forcing of Type 6 to Beijing area may be overwhelmed by the local atmospheric circulations (e.g. sea-breeze circulation and plain-mountain breeze circulation) in the idealized simulations with intense insolation, which may lead to the failure simulation of PBL structure for Type 6. Despite this discrepancy, the simulated BLH variations of other six synoptic patterns show good agreement with the variations of observed BLH, which provides a basis for using the simulation results of these six types to unravel the possible mechanisms affecting PBL structure. For these six synoptic types, the simulated BLH of Types 3 and 7 is significantly higher than that of Types 1, 2, 4, and 5 (Fig. 10).

Figure 11 shows the cross sections of simulated PT from Beijing to the coastline of Bohai sea. For Types 1 and 2, the southeasterly and easterly PBL winds could bring the cool marine air from the Bohai sea to Beijing, leading to cool the PBL over Beijing in the afternoon (Figs. 11a-b, 6a, and S5). Such cold advections associated with these two synoptic types could be partially responsible for the observed cool anomalies within PBL (Figs. 9a and 9b). And when the cool of PBL strengthens the thermal contrast between PBL (cold) and its upper level (warm), the growth of PBL could be suppressed, leading to exacerbate the air pollution there.

In contrary, warm anomalies are found in the afternoon within the lower part of troposphere for Types 3 and 4 (Figs. 9c and 9d), which may be caused by the westerly warm advections from the mountains (Figs. 11c-d, and S6). Since the mountains act as elevated heat sources in the afternoon and warm the adjacent air (Fig. S6), in the presence of westerly winds above the mountains, the warmer air could be transported to the plain regions of Beijing (Figs. 11c-d, and S6), imposing the warm anomalies

已删除:

已删除:

已删除: s

已删除: must

已删除:

on the PBL there. When the warm anomaly is stronger above PBL than within PBL, the development of PBL could be suppressed.

For Type 5, the cold advection within PBL and the warm advection aloft develop simultaneously over Beijing in the afternoon (Fig. 11e), strengthening the thermal inversion capping the PBL top and suppressing the growth of the PBL. Such a combination of cold and warm advections could be partly responsible for the relatively low BLH associated with Type 5 (Fig. 9e). The simultaneous presence of cold advection and warm advection also could be found in the simulated cross section of Type 7, but it is less prominent. As illustrated in Figs. 5g and 6a, under the synoptic conditions of Type 7, the synoptic forcing (northerly winds) within PBL do not support the advection of marine air from Bohai sea to Beijing, the simulated cold advection to Beijing is more likely to be induced by the local sea-breeze circulation.

In short, in addition to cloudiness, the results of idealized simulations demonstrate that the cold/warm advection induced by the synoptic forcing can also modulate the PBL structure in Beijing in the afternoon. With favorable thermal conditions in the summertime, the local atmospheric circulations (e.g., mountain-plain breeze, sea-land breeze) may be in place and superimposed on the large-scale synoptic advection, influencing the PBL structure in Beijing (Hu et al., 2014; Miao et al., 2015b).

4 Conclusions

In this study, seven different synoptic patterns during the summer in Beijing were identified using the T-PCA method and NCEP-FNL reanalysis data from 2011 to 2014. Their relationships with aerosol pollution and the PBL structure were comprehensively investigated using collocated long-term $PM_{2.5}$ measurements and fine-resolution soundings in Beijing.

The climatological diurnal cycle of the BLH, revealed by thrice-daily soundings (at 0800, 1400, and 2000 BJT) shows that the BLH reaches a maximum in the afternoon and is anti-correlated with the near-surface $PM_{2.5}$ concentration. In addition, daily aerosol pollution is significantly anti-correlated with the BLH at 1400 BJT. The correlation analysis between the BLH and local meteorological parameters

34

shows that in the afternoon, the BLH is negatively correlated with CLD and RH2. Thus, heavy aerosol pollution events frequently occur under cloudy conditions with high RH2 and low BLH.

By classifying the summertime 925-hPa GH fields over the Beijing-Tianjin-Hebei region (43°N-47°N, 112°E-125°E), three types of synoptic patterns favoring the occurrence of heavy aerosol pollution were identified, accounting for 67% of the total. At the 925-hPa level, these three synoptic types were characterized by high pressure systems located to the east or southeast of Beijing, leading to southerly PBL winds in Beijing. These southerly PBL winds favor the transport of pollutants from the surrounding southern industrial cities (e.g., Baoding, Shijiazhuang, and Cangzhou) to Beijing. Therefore, the horizontal transport of pollutants induced by the synoptic forcing may be one of the most important factor affecting the air quality of Beijing in summer. In the vertical dimension, these three synoptic types were characterized by a relatively low BLH at 1400 BJT, which may be highly associated with the relatively high CLD. The presence of cloud would reduce the solar radiation reaching land surface, and then suppress the development of PBL during the daytime. The similar impacts on the surface solar radiation can be induced by aerosols within PBL. Besides, the absorbing aerosols could heat the atmosphere, leading to a more stable and shallower PBL during the daytime.

In addition to the cloudiness and aerosols within PBL, the large-scale atmospheric advection within the PBL may play an important role in modulating the development of the PBL, which were examined by idealized simulations. In the afternoon, cold advection from the south within the PBL, induced by large-scale synoptic forcing, could decrease the PBL temperature and strengthen the thermal inversion above the PBL, thus suppressing the development of the PBL. Moreover, when warm advection appears simultaneously at the top level of the PBL, the suppression of the PBL is intensified. The suppression of PBL induced by the large-scale atmospheric advection under certain synoptic type, therefore, may also play a role in modulating the development of PBL in Beijing. These factors/processes combined tend to stabilize the daytime PBL over Beijing in the afternoon, which is schematically summarized in Fig. 12.

Although this study focuses on the daytime PBL structure, the nocturnal PBL also significantly affects the air quality at hourly to diurnal scales through the intermittent turbulence, which also cannot be ignored. The structure of nocturnal PBL is primarily determined by (stull, 1988; Salmond and

35

Mckendry, 2005). The nocturnal PBL may range from fully turbulent to intermittently turbulent or even non-turbulent at a variety of heights, temporal scales and spatial locations, which was largely induced by complex interactions between the static stability of the atmosphere and those processes (i.e. wind shear from synoptic patterns, terrain induced flows, low-level jets) that govern mechanical generation of turbulence. This makes it very difficult for the observation of large-scale atmospheric advection, investigation of the PBL-synoptic pattern interaction, transport pathways and dispersion of pollutants in the NBL, particular in regions of complex terrain such as Beijing. To fully understand the impacts of PBL on air quality in Beijing, more attention should be paid to the nocturnal PBL in the future.

Besides, although the important impacts of large-scale synoptic forcing on PBL structures and air quality in Beijing during the summer have been emphasized in this study, the important roles of local atmospheric circulations on the modulation of the PBL structure and air pollution cannot be overlooked. The presence of aerosols may also play a role in modifying PBL structures and processes, which warrants further study and will form the basis of our future work.

References

Abdi, H. and Williams, L. J.: Principal component analysis, Wiley Interdiscip. Rev. Comput. Stat., 2(4), 433–459, doi:10.1002/wics.101, 2010.

36

Bernaards, C. A. and Jennrich, R. I.: Gradient projection algorithms and software for arbitrary rotation criteria in factor analysis, Educ. Psychol. Meas., 65(5), 676–696, doi:10.1177/0013164404272507, 2005.

5   Chan, C. K. and Yao, X.: Air pollution in mega cities in China, Atmos. Environ., 42(1), 1–42, doi:10.1016/j.atmosenv.2007.09.003, 2008.

Chen, F. and Dudhia, J.: Coupling an Advanced Land Surface–Hydrology Model with the Penn State–NCAR MM5 Modeling System. Part I: Model Implementation and Sensitivity, Mon. Weather Rev., 129(4), 569–585, doi:10.1175/1520-0493(2001)129<0587:CAALSH>2.0.CO;2, 2001.

Chen, Y., Zhao, C., Zhang, Q., Deng, Z., Huang, M., and Ma, X.: Aircraft study of mountain chimney
10   effect of Beijing, China, J. Geophys. Res. Atmos., 114(8), 1–10, doi:10.1029/2008JD010610, 2009.

Chen, Z. H., Cheng, S. Y., Li, J. B., Guo, X. R., Wang, W. H. and Chen, D. S.: Relationship between atmospheric pollution processes and synoptic pressure patterns in northern China, Atmos. Environ., 42(24), 6078–6087, doi:10.1016/j.atmosenv.2008.03.043, 2008.

Chung, A., Chang, D. P. Y., Kleeman, M. J., Perry, K. D., Cahill, T. A., Dutcher, D., McDougall, E. M.,
15   and Stroud, K.: Comparison of real-time instruments used to monitor airborne particulate matter, J. Air Waste Manage. Assoc., 51(1), 109–120, doi:10.1080/10473289.2001.10464254, 2001.

Craven, J. P., Jewell, R. E., and Brooks, H. E.: Comparison between observed convective cloud-base heights and lifting condensation level for two different lifted parcels, Weather Forecast., 885–890, doi:10.1175/1520-0434(2002)017<0885:CBOCCB>2.0.CO;2, 2002.

20   De Wekker, S. F. J.: Observational and numerical evidence of depressed convective boundary layer heights near a mountain base, J. Appl. Meteorol. Climatol., 47(4), 1017–1026, doi:10.1175/2007JAMC1651.1, 2008.

Ding, A. J., Huang, X., Nie, W., Sun, J. N., Kerminen, V.-M., Petäjä, T., Su, H., Cheng, Y. F., Yang, X.-Q., Wang, M. H., Chi, X. G., Wang, J. P., Virkkula, A., Guo, W. D., Yuan, J., Wang, S. Y.,
25   Zhang, R. J., Wu, Y. F., Song, Y., Zhu, T., Zilitinkevich, S., Kulmala, M., and Fu, C. B.: Black carbon enhances haze pollution in megacities in China, Geophys. Res. Lett., 43, 1–7, doi:10.1002/2016GL067745, 2016.

Garratt, J.: Review: the atmospheric boundary layer, Earth-Science Rev., 37, 89–134, doi:10.1016/0012-8252(94)90026-4, 1994.

30   Gao, Y., Zhang, M., Liu, Z., Wang, L., Wang, P., Xia, X., Tao, M. and Zhu, L.: Modeling the feedback between aerosol and meteorological variables in the atmospheric boundary layer during a severe fog–haze event over the North China Plain, Atmos. Chem. Phys., 15(8), 4279–4295, doi:10.5194/acp-15-4279-2015, 2015.

Guo, J. P., Zhang, X. Y., Wu, Y. R., Zhaxi, Y., Che, H. Z., La, B., Wang, W., and Li, X. W.: Spatio-
35   temporal variation trends of satellite-based aerosol optical depth in China during 1980-2008, Atmos. Environ., 45(37), 6802–6811, doi:10.1016/j.atmosenv.2011.03.068, 2011.

Guo, J., Niu, T., Wang, F., Deng, M., and Wang, Y.: Integration of multi-source measurements to monitor sand-dust storms over North China: A case study, Acta Meteorol. Sin., 27(4), 566–576, doi:10.1007/s13351-013-0409-z, 2013.

40   Guo, J., Miao, Y., Zhang, Y., Liu, H., Li, Z., Zhang, W., He, J., Lou, M., Yan, Y., Bian, L., and Zhai, P.: The climatology of planetary boundary layer height in China derived from radiosonde and reanalysis data, Atmos. Chem. Phys., 16, 13309–13319, 10.5194/acp-16-13309-2016, 2016.

37

Guo, S., Hu, M., Zamora, M. L., Peng, J., Shang, D., Zheng, J., Du, Z., Wu, Z., Shao, M., Zeng, L., Molina, M. J., and Zhang, R.: Elucidating severe urban haze formation in China, Proc. Natl. Acad. Sci. U. S. A., 111(49), 17373–17378, doi:10.1073/pnas.1419604111, 2014.

Han, T., Liu, X., Zhang, Y., Qu, Y., Zeng, L., Hu, M., and Zhu, T.: Role of secondary aerosols in haze formation in summer in the Megacity Beijing, J. Environ. Sci., 31, 51–60, doi:10.1016/j.jes.2014.08.026, 2015.

He, K., Yang, F., Ma, Y., Zhang, Q., Yao, X., Chan, C. K., Cadle, S., Chan, T., and Mulawa, P.: The characteristics of $PM_{2.5}$ in Beijing, China, Atmos. Environ., 35(29), 4959–4970, doi:10.1016/S1352-2310(01)00301-6, 2001.

Hong, S.-Y., Noh, Y. and Dudhia, J.: A New Vertical Diffusion Package with an Explicit Treatment of Entrainment Processes, Mon. Weather Rev., 134(9), 2318–2341, doi:10.1175/MWR3199.1, 2006.

Hu, X., Ma, Z., Lin, W., Zhang, H., Hu, J., Wang, Y., Xu, X., Fuentes, J. D., and Xue, M.: Impact of the Loess Plateau on the atmospheric boundary layer structure and air quality in the North China Plain : A case study, Sci. Total Environ., 499, 228–237, doi:10.1016/j.scitotenv.2014.08.053, 2014.

Huang, R.-J., Zhang, Y., Bozzetti, C., Ho, K.-F., Cao, J.-J., Han, Y., Daellenbach, K. R., Slowik, J. G., Platt, S. M., Canonaco, F., Zotter, P., Wolf, R., Pieber, S. M., Bruns, E. a., Crippa, M., Ciarelli, G., Piazzalunga, A., Schwikowski, M., Abbaszade, G., Schnelle-Kreis, J., Zimmermann, R., An, Z., Szidat, S., Baltensperger, U., Haddad, I. El, and Prévôt, A. S. H.: High secondary aerosol contribution to particulate pollution during haze events in China, Nature, 514, doi:10.1038/nature13774, 2014.

Huth, R.: An intercomparison of computer-assisted circulation classification methods, Int. J. Climatol., 16(8), 893–922, doi:10.1002/(SICI)1097-0088(199608)16:8<893::AID-JOC51>3.0.CO;2-Q, 1996.

Huth, R.: A circulation classification scheme applicable in GCM studies, Theor. Appl. Climatol., 67, 1–18, doi:10.1007/s007040070012, 2000.

Huth, R., Beck, C., Philipp, A., Demuzere, M., Ustrnul, Z., Cahynová, M., Kyselý, J., and Tveito, O. E.: Classifications of atmospheric circulation patterns: Recent advances and applications, Ann. N. Y. Acad. Sci., 1146, 105–152, doi:10.1196/annals.1446.019, 2008.

Iacono, M. J., Delamere, J. S., Mlawer, E. J., Shephard, M. W., Clough, S. A. and Collins, W. D.: Radiative forcing by long-lived greenhouse gases: Calculations with the AER radiative transfer models, J. Geophys. Res., 113(D13), D13103, doi:10.1029/2008JD009944, 2008.

Kim, Y., Kim, S.-W., and Yoon, S.-C.: Observation of new particle formation and growth under cloudy conditions at Gosan Climate Observatory, Korea, Meteorol Atmos Phys, 126, 81–90, doi: 10.1007/s00703-014-0336-2, 2014.

Kusaka, H., Kondo, H., Kikegawa, Y. and Kimura, F.: A Simple Single-Layer Urban Canopy Model For Atmospheric Models: Comparison With Multi-Layer And Slab Models, Boundary-Layer Meteorol., 101(3), 329–358, doi:10.1023/A:1019207923078, 2001.

Li, J., Chen, H., Li, Z., Wang, P., Cribb, M., and Fan, X.: Low-level temperature inversions and their effect on aerosol condensation nuclei concentrations under different large-scale synoptic circulations, Adv. Atmos. Sci., 32(7), 898–908, doi:10.1007/s00376-014-4150-z, 2015.

Li, Z., Xia, X., Cribb, M., Mi, W., Holben, B., Wang, P., Chen, H., Tsay, S.-C., Eck, T. F., Zhao, F., Dutton, E. G. and Dickerson, R. E.: Aerosol optical properties and their radiative effects in northern China, J. Geophys. Res., 112(D22), 1–11, doi:10.1029/2006JD007382, 2007.

38

Li, Z., Lau, W. K.-M., Ramanathan, V., Wu, G., Ding, Y., Manoj, M. G., Liu, J., Qian, Y., Li, J., Zhou, T., Fan, J., Rosenfeld, D., Ming, Y., Wang, Y., Huang, J., Wang, B., Xu, X., Lee, S.-S., Cribb, M., Zhang, F., Yang, X., Zhao, C., Takemura, T., Wang, K., Xia, X., Yin, Y., Zhang, H., Guo, J., Zhai, P. M., Sugimoto, N., Babu, S. S. and Brasseur, G. P.: Aerosol and monsoon climate interactions over Asia, Rev. Geophys., 119–161, doi:10.1002/2015RG000500, 2016.

Liu, S. and Liang, X. Z.: Observed diurnal cycle climatology of planetary boundary layer height, J. Clim., 23(21), 5790–5809, doi:10.1175/2010JCLI3552.1, 2010.

Liu, S., Liu, Z., Li, J., Wang, Y., Ma, Y., Sheng, L., Liu, H., Liang, F., Xin, G., and Wang, J.: Numerical simulation for the coupling effect of local atmospheric circulations over the area of Beijing, Tianjin and Hebei Province, Sci. China Ser. D Earth Sci., 52(3), 382–392, doi:10.1007/s11430-009-0030-2, 2009.

Liu, X. G., Li, J., Qu, Y., Han, T., Hou, L., Gu, J., Chen, C., Yang, Y., Liu, X., Yang, T., Zhang, Y., Tian, H., and Hu, M.: Formation and evolution mechanism of regional haze: A case study in the megacity Beijing, China, Atmos. Chem. Phys., 13(9), 4501–4514, doi:10.5194/acp-13-4501-2013, 2013.

Liu, X., Yan, L., Yang, P., Yin, Z. Y. and North, G. R.: Influence of Indian summer monsoon on aerosol loading in East Asia, J. Appl. Meteorol. Climatol., 50(3), 523–533, doi:10.1175/2010JAMC2414.1, 2011.

Liu, Z., Wang, Y., Hu, B., Ji, D., Zhang, J., Wu, F., Wan, X. and Wang, Y.: Source appointment of fine particle number and volume concentration during severe haze pollution in Beijing in January 2013, Environ. Sci. Pollut. Res., 23(7), 6845–6860, doi:10.1007/s11356-015-5868-6, 2016.

Miao, Y., Liu, S., Zheng, Y., Wang, S., and Chen, B.: Numerical study of the effects of topography and urbanization on the local atmospheric circulations over the Beijing-Tianjin-Hebei, China, Adv. Meteorol., 2015, 1–16, doi:10.1155/2015/397070, 2015a.

Miao, Y., Hu, X.-M., Liu, S., Qian, T., Xue, M., Zheng, Y., and Wang, S.: Seasonal variation of local atmospheric circulations and boundary layer structure in the Beijing-Tianjin-Hebei region and implications for air quality, J. Adv. Model. Earth Syst., 7(1), 1–25, doi:10.1002/2015MS000522, 2015b.

Miao, Y., Liu, S., Zheng, Y., and Wang, S.: Modeling the feedback between aerosol and boundary layer processes: a case study in Beijing, China, Environ. Sci. Pollut. Res., 23(4), 3342–3357, doi:10.1007/s11356-015-5562-8, 2016.

Miller, S. T. K.: Sea breeze: Structure, forecasting, and impacts, Rev. Geophys., 41(3), 1011, doi:10.1029/2003RG000124, 2003.

Niu, F., Li, Z., Li, C., Lee, K. H., and Wang, M.: Increase of wintertime fog in China: Potential impacts of weakening of the Eastern Asian monsoon circulation and increasing aerosol loading, J. Geophys. Res. Atmos., 115(19), 1–12, doi:10.1029/2009JD013484, 2010.

Peng, J., Hu, M., Guo, S., Du, Z., Zheng, J., Shang, D., Levy Zamora, M., Zeng, L., Shao, M., Wu, Y.-S., Zheng, J., Wang, Y., Glen, C. R., Collins, D. R., Molina, M. J. and Zhang, R.: Markedly enhanced absorption and direct radiative forcing of black carbon under polluted urban environments, Proc. Natl. Acad. Sci., 113(16), 4266–4271, doi:10.1073/pnas.1602310113, 2016.

Philipp, A., Bartholy, J., Beck, C., Erpicum, M., Esteban, P., Fettweis, X., Huth, R., James, P., Jourdain, S., Kreienkamp, F., Krennert, T., Lykoudis, S., Michalides, S. C., Pianko-Kluczynska, K., Post, P.,

39

Álvarez, D. R., Schiemann, R., Spekat, A., and Tymvios, F. S.: Cost733cat - A database of weather and circulation type classifications, Phys. Chem. Earth, 35(9–12), 360–373, doi:10.1016/j.pce.2009.12.010, 2010.

Pu, B. and Dickinson, R. E.: Diurnal spatial variability of Great Plains summer precipitation related to the dynamics of the low-level jet, J. Atmos. Sci., 71, 1807–1817, doi:10.1175/JAS-D-13-0243.1, 2014.

Quan, J., Gao, Y., Zhang, Q., Tie, X., Cao, J., Han, S., Meng, J., Chen, P., and Zhao, D.: Evolution of planetary boundary layer under different weather conditions, and its impact on aerosol concentrations, Particuology, 11(1), 34–40, doi:10.1016/j.partic.2012.04.005, 2013.

Quan, J., Tie, X., Zhang, Q., Liu, Q., Li, X., Gao, Y., and Zhao, D.: Characteristics of heavy aerosol pollution during the 2012–2013 winter in Beijing, China, Atmos. Environ., 88, 83–89, doi:10.1016/j.atmosenv.2014.01.058, 2014.

Richman, M. B.: Obliquely rotated principal components: An improved meteorological map typing technique?, J. Appl. Meteorol., 20(10), 1145–1159, doi:10.1175/1520-0450(1981)020<1145:ORPCAI>2.0.CO;2, 1981.

Salmond, J. a. and McKendry, I. G.: A review of turbulence in the very stable nocturnal boundary layer and its implications for air quality, Prog. Phys. Geogr., 29(2), 171–188, doi:10.1191/0309133305pp442ra, 2005.

San Martini, F. M., Hasenkopf, C. A., and Roberts, D. C.: Statistical analysis of PM$_{2.5}$ observations from diplomatic facilities in China, Atmos. Environ., 110, 174–185, doi:10.1016/j.atmosenv.2015.03.060, 2015.

Seidel, D. J., Zhang, Y., Beljaars, A., Golaz, J.-C., Jacobson, A. R., and Medeiros, B.: Climatology of the planetary boundary layer over the continental United States and Europe, J. Geophys. Res. Atmos., 117(D17), 1–15, doi:10.1029/2012JD018143, 2012.

Stefan, S., Necula, C., and Georgescu, F.: Analysis of long-range transport of particulate matters in connection with air circulation over Central and Eastern part of Europe, Phys. Chem. Earth, 35(9–12), 523–529, doi:10.1016/j.pce.2009.12.008, 2010.

Stull, R. B.: An introduction to boundary layer meteorology, edited by R. B. Stull, Springer Netherlands, Dordrecht., 1988.

Sun, Y., Song, T., Tang, G., and Wang, Y.: The vertical distribution of PM$_{2.5}$ and boundary-layer structure during summer haze in Beijing, Atmos. Environ., 74, 413–421, doi:10.1016/j.atmosenv.2013.03.011, 2013.

Tang, G., Zhang, J., Zhu, X., Song, T., Münkel, C., Hu, B., Schäfer, K., Liu, Z., Zhang, J., Wang, L., Xin, J., Suppan, P., and Wang, Y.: Mixing layer height and its implications for air pollution over Beijing, China, Atmos. Chem. Phys., 16(4), 2459–2475, doi:10.5194/acp-16-2459-2016, 2016.

Tie, X., Zhang, Q., He, H., Cao, J., Han, S., Gao, Y., Li, X., and Jia, X. C.: A budget analysis of the formation of haze in Beijing, Atmos. Environ., 100, 25–36, doi:10.1016/j.atmosenv.2014.10.038, 2015.

Vogelezang, D. H. P. and Holtslag, A. A. M.: Evaluation and model impacts of alternative boundary-layer height formulations, Boundary-Layer Meteorol., 81(3–4), 245–269, doi:10.1007/BF02430331, 1996.

40

Wang, F., Chen, D. S., Cheng, S. Y., Li, J. B., Li, M. J., and Ren, Z. H.: Identification of regional atmospheric PM$_{10}$ transport pathways using HYSPLIT, MM5-CMAQ and synoptic pressure pattern analysis, Environ. Modell. Softw., 25(8), 927–934, doi:10.1016/j.envsoft.2010.02.004, 2010.

Wang, H., Xu, J., Zhang, M., Yang, Y., Shen, X., Wang, Y., Chen, D., and Guo, J.: A study of the meteorological causes of a prolonged and severe haze episode in January 2013 over central-eastern China, Atmos. Environ., 98, 146–157, doi:10.1016/j.atmosenv.2014.08.053, 2014.

Wang, L., Liu, Z., Sun, Y., Ji, D., and Wang, Y.: Long-range transport and regional sources of PM$_{2.5}$ in Beijing based on long-term observations from 2005 to 2010, Atmos. Res., 157, 37–48, doi:10.1016/j.atmosres.2014.12.003, 2015a.

Wang, L., Xin, J., Li, X., and Wang, Y.: The variability of biomass burning and its influence on regional aerosol properties during the wheat harvest season in North China, Atmos. Res., 157, 153–163, doi:10.1016/j.atmosres.2015.01.009, 2015b.

Wei, P., Cheng, S., Li, J. and Su, F.: Impact of boundary-layer anticyclonic weather system on regional air quality, Atmos. Environ., 45(14), 2453–2463, doi:10.1016/j.atmosenv.2011.01.045, 2011.

Wilde, N. P., Stull, R. B., and Eloranta, E. W.: The LCL zone and cumulus onset, J. Clim. Appl. Meteorol., 24(7), 640–657, doi:10.1175/1520-0450(1985)024<0640:TLZACO>2.0.CO;2, 1985.

Wu, G. X., Li, Z. Q., Fu, C. B., Zhang, X. Y., Zhang, R. Y., Zhang, R. H., Zhou, T. J., Li, J. P., Li, J. D., Zhou, D. G., Wu, L., Zhou, L. T., He, B., and Huang, R. H.: Advances in studying interactions between aerosols and monsoon in China, Sci. China Earth Sci., 59(1), 1–16, doi:10.1007/s11430-015-5198-z, 2016.

Yan, L., Liu, X., Yang, P., Yin, Z. Y. and North, G. R.: Study of the impact of summer monsoon circulation on spatial distribution of aerosols in East Asia based on numerical simulations, J. Appl. Meteorol. Climatol., 50(11), 2270–2282, doi:10.1175/2011JA, 2011.

Ye, X., Song, Y., Cai, X., and Zhang, H.: Study on the synoptic flow patterns and boundary layer process of the severe haze events over the North China Plain in January 2013, Atmos. Environ., 124, 129–145, doi:10.1016/j.atmosenv.2015.06.011, 2016.

Yoo, J.-M., Lee, Y.-R., Kim, D., Jeong, M.-J., Stockwell, W. R., Kundu, P. K., Oh, S.-M., Shin, D.-B., and Lee, S.-J.: New indices for wet scavenging of air pollutants (O$_3$, CO, NO$_2$, SO$_2$, and PM$_{10}$) by summertime rain, Atmos. Environ., 82, 226–237, doi:10.1016/j.atmosenv.2013.10.022, 2014.

Zhang, J. P., Zhu, T., Zhang, Q. H., Li, C. C., Shu, H. L., Ying, Y., Dai, Z. P., Wang, X., Liu, X. Y., Liang, A. M., Shen, H. X., and Yi, B. Q.: The impact of circulation patterns on regional transport pathways and air quality over Beijing and its surroundings, Atmos. Chem. Phys., 12(11), 5031–5053, doi:10.5194/acp-12-5031-2012, 2012.

Zhang, L., Liao, H., and Li, J.: Impacts of Asian summer monsoon on seasonal and interannual variations of aerosols over eastern China, J. Geophys. Res., 115, 1–21, doi:10.1029/2009JD012299, 2010.

Zhang, R., Jing, J., Tao, J., Hsu, S. C., Wang, G., Cao, J., Lee, C. S. L., Zhu, L., Chen, Z., Zhao, Y., and Shen, Z.: Chemical characterization and source apportionment of PM$_{2.5}$ in Beijing: Seasonal perspective, Atmos. Chem. Phys., 13(14), 7053–7074, doi:10.5194/acp-13-7053-2013, 2013.

Zhang, R., Wang, G., Guo, S., Zamora, M. L., Ying, Q., Lin, Y., Wang, W., Hu, M. and Wang, Y.: Formation of Urban Fine Particulate Matter, Chem. Rev., 115(10), 3803–3855, doi:10.1021/acs.chemrev.5b00067, 2015.
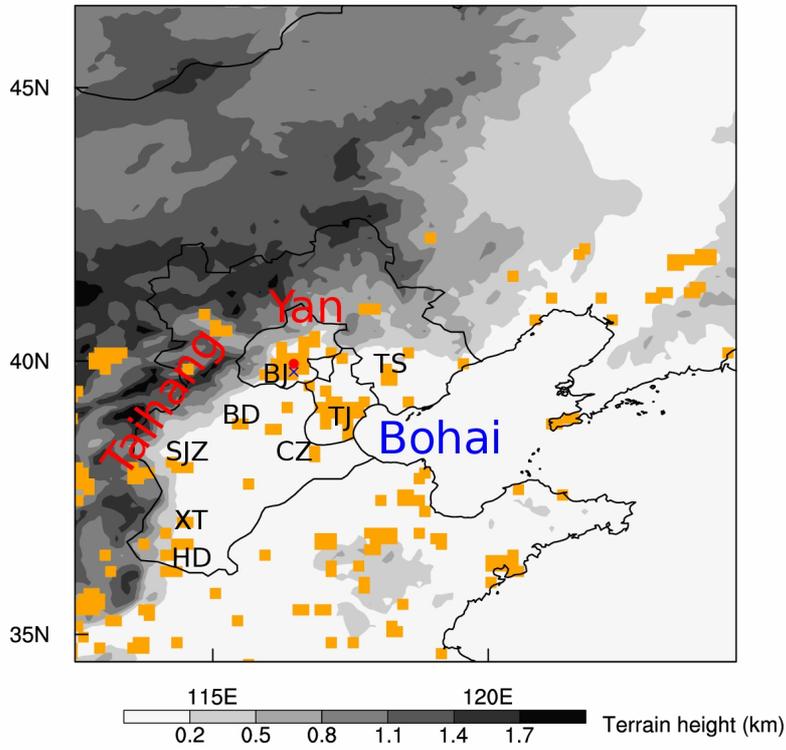
41

已删除: (January 2013)

已删除: Zhang, H., Wang, Y., Hu, J., Ying, Q., and Hu, X.-M.: Relationships between meteorological parameters and criteria air pollutants in three megacities in China, Environ. Res., 140, 242–254, doi:10.1016/j.envres.2015.04.004, 2015.

Zhang, W., Guo, J., Miao, Y., Liu, H., Zhang, Y., Li, Z., and Zhai, P.: Planetary boundary layer height from CALIOP compared to radiosonde over China, Atmos. Chem. Phys., 16(15), 9951–9963, doi:10.5194/acp-16-9951-2016, 2016.

Zhang, Y. L. and Cao, F.: Fine particulate matter ($PM_{2.5}$) in China at a city level, Sci. Rep., 5(2014), 14884, doi:10.1038/srep14884, 2015.

Zhang, Z., Zhang, X., Gong, D., Quan, W., Zhao, X., Ma, Z., and Kim, S. J.: Evolution of surface O_3 and $PM_{2.5}$ concentrations and their relationships with meteorological conditions over the last decade in Beijing, Atmos. Environ., 108, 67–75, doi:10.1016/j.atmosenv.2015.02.071, 2015.

Zhao, Y., Zhang, Q., Du, Y., Jiang, M., and Zhang, J.: Objective analysis of circulation extremes during the 21 July 2012 torrential rain in Beijing, Acta Meteorol. Sin., 27(5), 626–635, doi:10.1007/s13351-013-0507-y, 2013.

Zhu, J., Liao, H. and Li, J.: Increases in aerosol concentrations over eastern China due to the decadal-scale weakening of the East Asian summer monsoon, Geophys. Res. Lett., 39(9), 1–6, doi:10.1029/2012GL051428, 2012.

Zhu, L., Huang, X., Shi, H., Cai, X., and Song, Y.: Transport pathways and potential sources of PM_{10} in Beijing, Atmos. Environ., 45(3), 594–604, doi:10.1016/j.atmosenv.2010.10.040, 2011.

Zhu, P. and Albrecht, B.: A theoretical and observational analysis on the formation of fair-weather cumuli, J. Atmos. Sci., 59(12), 1983–2005, doi:10.1175/1520-0469(2002)059<1983:ATAOAO>2.0.CO;2, 2002.

已删除: -

已删除: Zhao, X., Zhuang, G., Wang, Z., Sun, Y., Wang, Y., and Yuan, H.: Variation of sources and mixing mechanism of mineral dust with pollution aerosol—revealed by the two peaks of a super dust storm in Beijing, Atmos. Res., 84(3), 265–279, doi:10.1016/j.atmosres.2006.08.005, 2007.

已设置格式: 字体:(默认) Lantinghei TC Heavy, (中文) Lantinghei TC Heavy

42

Fig. 1. Spatial distribution of terrain height of the North China Plain. Superimposed are the locations of the U.S. Embassy air quality station (39.95°N, 116.47°E, the red dot) and the Beijing meteorological station (39.80°N, 116.47°E, the blue cross). Urbanized areas based on MODIS 2012 data are shown in orange. The locations of Beijing (BJ) and adjacent industrial cities are written in black text and include Tianjin (TJ), Tangshan (TS), Baoding (BD), Cangzhou (CZ), Shijiazhuang (SJZ), Xingtai (XT), and Handan (HD).
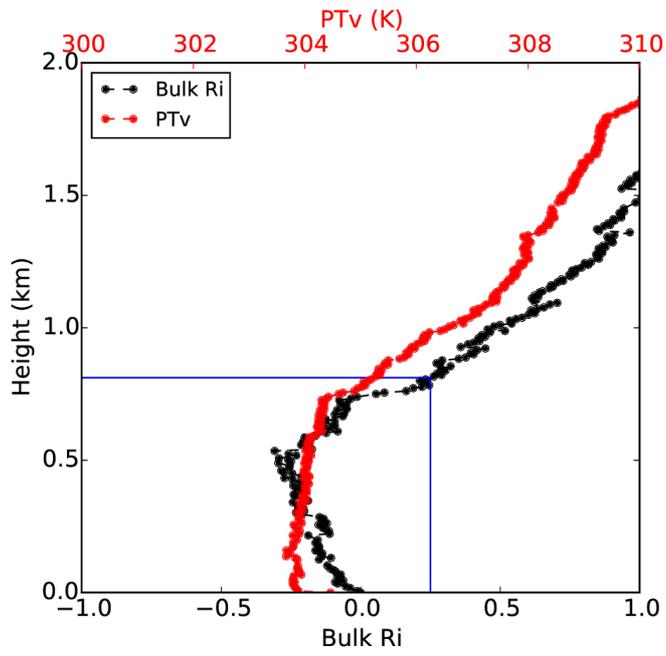
Fig. 2. Vertical profiles of the bulk Richardson number (Ri, in black) and virtual potential temperature (PTv, in red) based on L-band sounding observations made in Beijing on 30 June 2013 at 1400 BJT. The boundary layer height is the height where Ri first reaches the value of 0.25 (the blue lines).

5

44
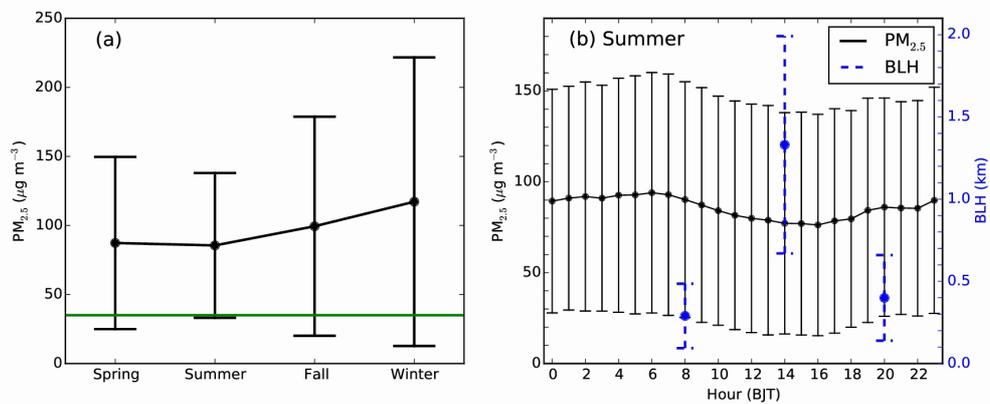
Fig. 3. (a) Seasonal variation of the daily averaged $PM_{2.5}$ concentration (the mean ± one standard deviation), and (b) diurnal cycle of the $PM_{2.5}$ concentration (the mean ± one standard deviation) in summer derived from hourly measurements made at the U.S. Embassy air quality station from 2011 to
5 2014. The green line in (a) shows the national standard level (35 μg m^{-3}). The diurnal cycle of the BLH (in blue, the mean ± one standard deviation) derived from summertime soundings in Beijing is shown in (b) on the right-hand ordinate.
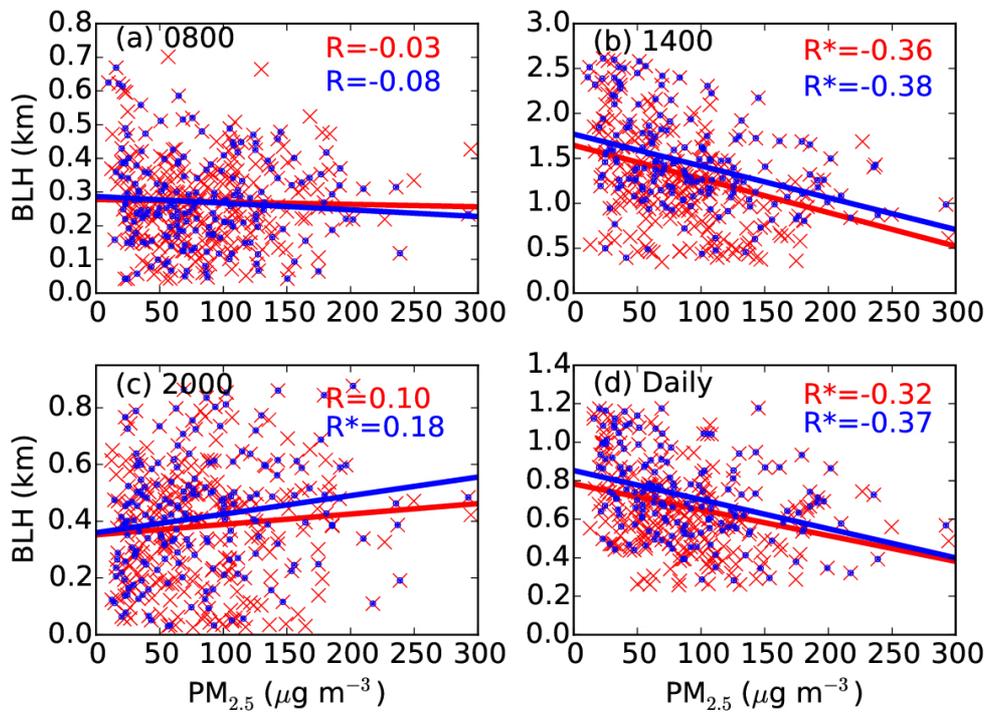
45

Fig. 4. The BLH as a function of daily PM$_{2.5}$ concentration at (a) 0800 BJT, (b) 1400 BJT, (c) 2000 BJT, and (d) averaged over the whole day (in red). BLHs greater than the 95th percentile value and less than the 5th percentile value are not included in the plots. The correlations between the PM$_{2.5}$ concentration and BLH without considering measurements made on rainy days are shown in blue. The correlation coefficients (R) are given in each panel, and the asterisks indicate values that are statistically significant ($p < 0.05$). The p-values were calculated based on the student's t-distribution.

已设置格式: 字体:加粗

已删除: ,

46
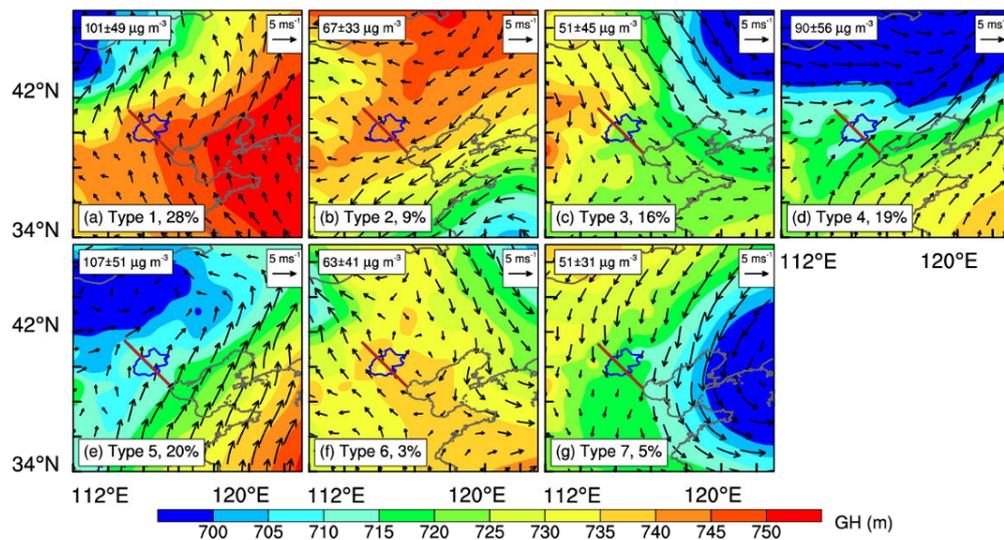
Fig. 5. 925-hPa geopotential height (GH) fields (colored areas) and wind vector fields (arrows) in summer from 2011 to 2014 for the seven synoptic patterns: (a) Type 1, (b) Type 2, (c) Type 3, (d) Type 4, (e) Type 5, (f) Type 6, and (g) Type 7. The occurrence frequency of each synoptic pattern is given in the bottom left of each panel and the $PM_{2.5}$ concentration (the mean ± one standard deviation) is shown in the top left of each panel. The location of the Beijing metropolitan area is outlined in blue near the center of each panel. The red lines cutting through the Beijing metropolitan area in (a-g) indicate the location of the cross-sections shown in Fig. 11.

47
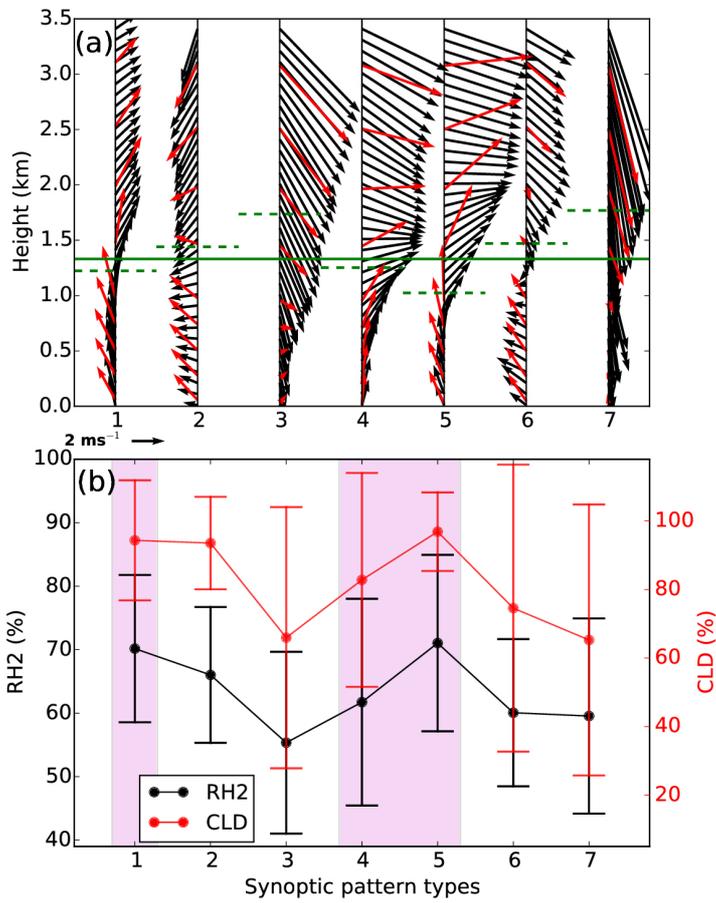
Fig. 6. (a) Average wind vector profiles at 1400 BJT and (b) observed daily RH2 and CLD at 1400 BJT (mean ± one standard deviation) associated with the seven types of synoptic pattern. In (a), the wind vectors derived from soundings are denoted by black vectors and those from the NCEP-FNL reanalysis are in red. The green solid line shows the seasonal mean BLH and the dashed green lines represent the mean BLH for each synoptic pattern type. Note that the wind vector profiles from the NCEP-FNL reanalysis were derived by interpolating the values from the four nearest grids.

48
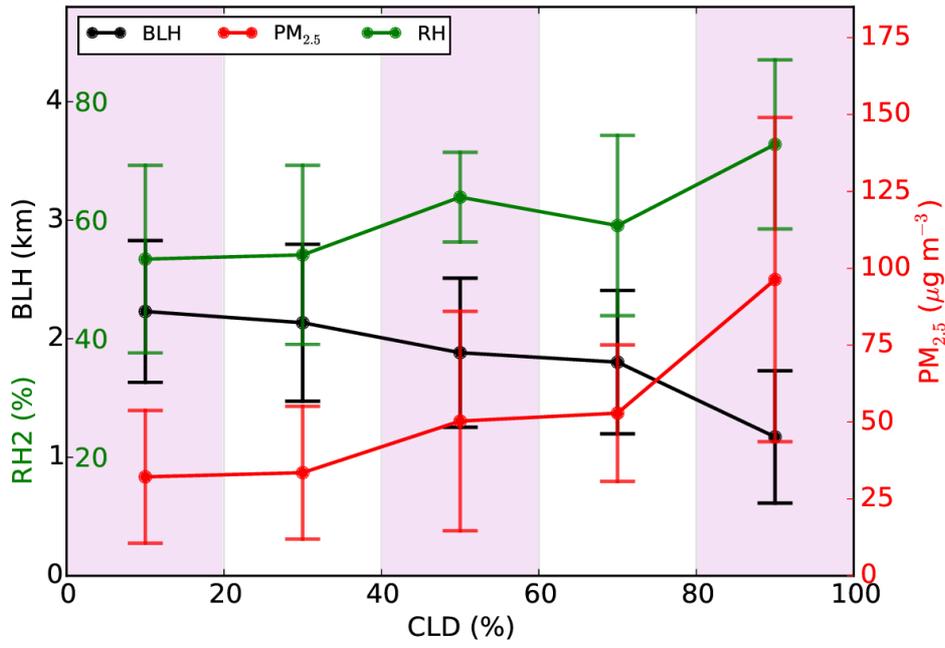
Fig. 7. The BLH at 1400 BJT (in black), daily RH2 (in green), and daily PM$_{2.5}$ concentration (in red) as a function of CLD at 1400 BJT. Mean values ± one standard deviation are shown. The bin size is 20%.

5

49
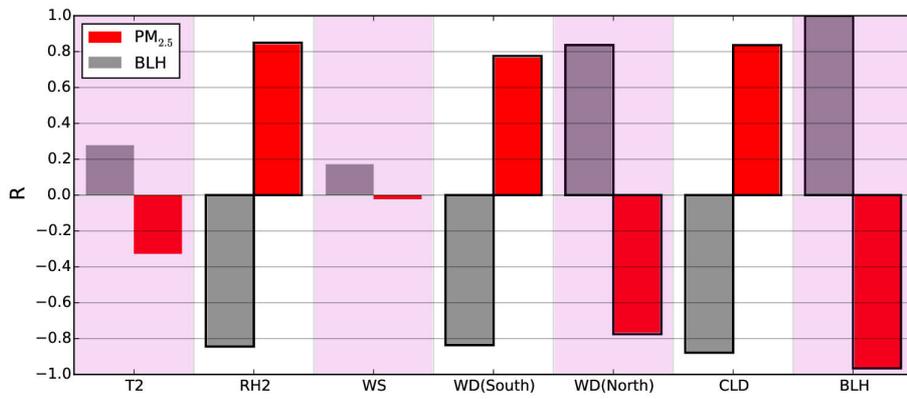
Fig. 8. Correlations (R) between the mean values of PM$_{2.5}$ concentration and meteorological parameters for the different synoptic patterns, including (from left to right) 2-m temperature (T2), 2-m relative humidity (RH2), wind speed at the 925-hPa level (WS), south- and north- wind frequencies at the 925h-
5   hPa level (WD), total cloud cover at 1400 BJT (CLD), and the BLH at 1400 BJT. The grey bars represent the correlations between BLH and these meteorological parameters. Bars outlined in thick black lines indicate correlation coefficients (R) that are statistically significant ($p < 0.05$). Note that the R is calculated based on the seven pairs of mean values for different synoptic patterns.

已删除: of

50

Fig. 9. Vertical profiles of potential temperature (PT) at 1400 BJT associated with the seven types of synoptic pattern derived from soundings (red lines). Solid lines indicate average values and shaded areas show the uncertainty range (the mean ± one standard deviation). Green solid lines represent the summer averaged BLH and green dashed lines represent the average BLH for each synoptic type. The PT anomaly (subtracted from the summer averaged PT profile) for each synoptic type was also given by the blue dash-lines in each panel.

51

Fig. 10. The simulated BLH at 1400 BJT (in black) and observed BLH at 1400 BJT (in red) over Beijing were shown as function of synoptic types.
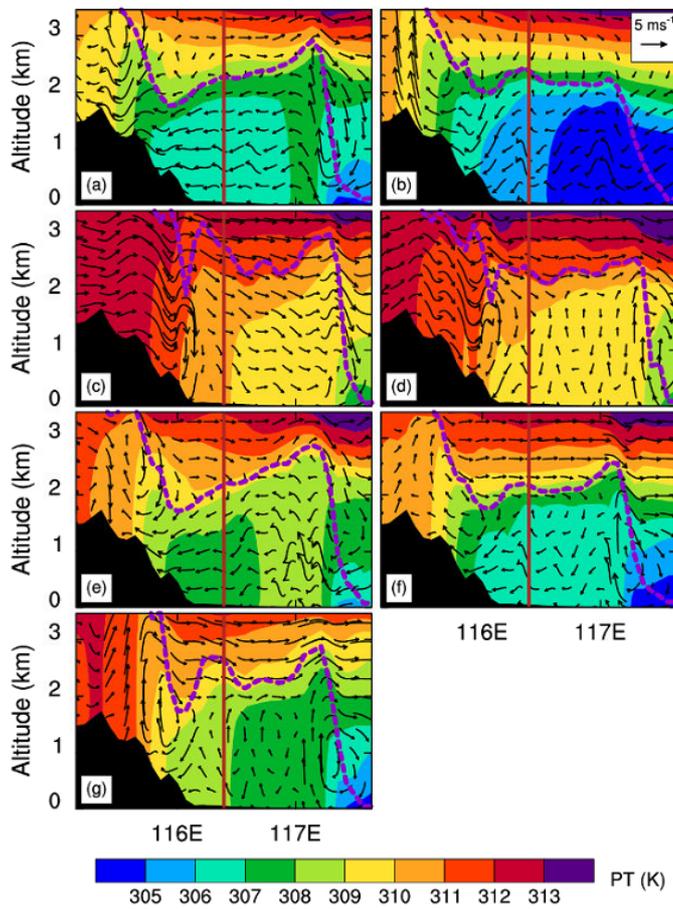
5

Fig. 11. Vertical cross-sections of the PT and wind vectors at 1400 BJT for the seven synoptic pattern types: (a) Type 1, (b) Type 2, (c) Type 3, (d) Type 4, (e) Type 5, (f) Type 6, and (g) Type 7. The vertical wind component is multiplied by a factor of 30 when plotting the wind vector fields. The black area on the left side of each panel shows the terrain. The red line shows the location of the sounding station in Beijing. The violet dashed line marks the BLH estimated using the Ri method. The location of the cross-section is shown by the black line in Fig. 5a.
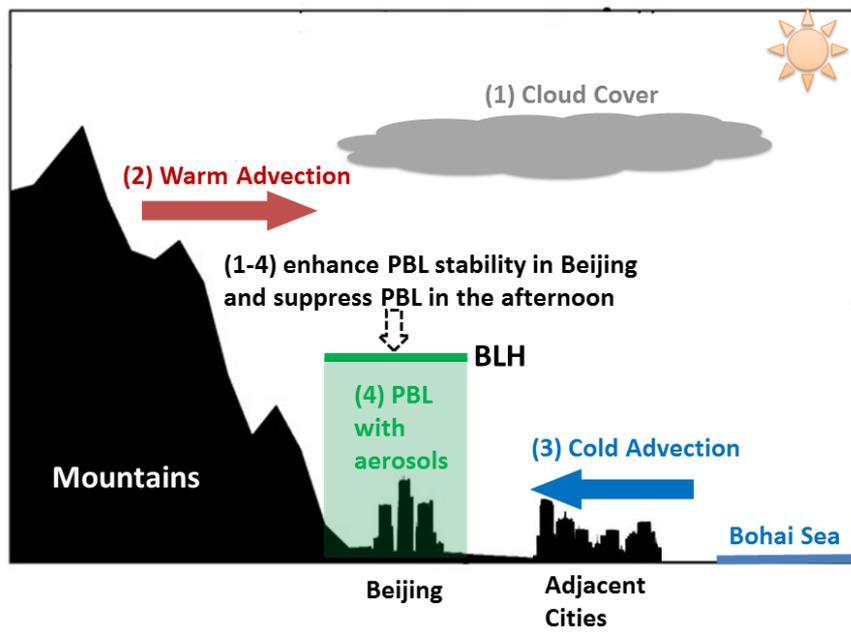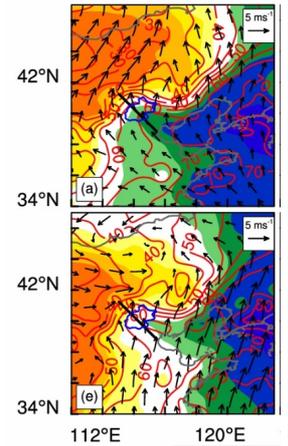
Fig. 12. Schematic diagram of factors/processes suppressing PBL over Beijing in the afternoon, including (1) high cloud cover, (2) westerly warm advection above PBL, (3) southerly cold advection within PBL, and (4) aerosols within PBL